Short-lived, fast erosional exhumation of the internal western Alps during the late early Oligocene: Constraints from geothermochronology of pro- and retro-side foreland basin sediments

Sébastien Jourdan[1], Matthias Bernet[1], Pierre Tricart[1], Elizabeth Hardwick[1], Jean-Louis Paquette[2], Stéphane Guillot[1], Thierry Dumont[1], and Stéphane Schwartz[1]

[1]ISTERRE, UNIVERSITÉ DE GRENOBLE 1, CNRS, 1381 RUE DE LA PISCINE, F-38041 GRENOBLE, FRANCE

[2]LABORATOIRE MAGMAS AND VOLCANS, UMR6524 CNRS AND UNIVERSITÉ BLAISE PASCAL, 5 RUE KESSLER, F-63038 CLERMONT-FERRAND, FRANCE

ABSTRACT

Apatite and zircon fission-track analysis and single zircon fission-track–U/Pb double dating of Oligocene to Miocene pro- and retro-side foreland basin sedimentary rocks provide evidence for short-lived but fast erosional exhumation of at least 1.5–2 km/m.y. in the internal western Alps between ca. 30 and 28 Ma. This period of fast erosion is seen as a result of rapid surface uplift coupled with increasing orographic precipitation during this phase of orogenesis. Surface uplift may have been caused and sustained by different plate-tectonic processes such as a change in convergence direction, intermediate-depth slab breakoff, and emplacement of the Ivrea body during continental collision. The occurrence of contemporaneous volcanic activity on the pro-side of the western Alps on the subducting European plate between ca. 36 Ma and 30 Ma is seen in connection with slab rollback of the Apennine slab and upwelling of hot mantle material beneath the western Alps. Single zircon double dating shows that the exhumational signal in the detrital thermochronologic data is not compromised by volcanically derived zircons, as volcanic grains can be identified and removed from the zircon fission-track data set to obtain a pure exhumational signal. The signal of fast exhumation is observed in the zircon fission-track data of the pro-side foreland basin and in the apatite fission-track data and published ^{40}Ar-^{39}Ar data in the retro-side foreland basin. During late Oligocene times, erosion rates slowed down to rates similar to present-day erosion rates in the western Alps.

LITHOSPHERE; v. 5; no. 2; p. 211–225; GSA Data Repository Item 2013100 | Published online 25 February 2013 doi: 10.1130/L243.1

INTRODUCTION

The Oligocene is a key period in the evolution of the western Alps during which the mountain belt evolved from an accretionary wedge (Late Cretaceous–Eocene; e.g., Handy et al., 2010, and references therein) to a relatively high-elevation mountain belt, similar to the central Alps today (e.g., Pfiffner, 1986; Kühni and Pfiffner, 2001; Garzanti and Malusà, 2008; Campani et al., 2012). Studying the sediments and sedimentary rocks deposited in basins adjacent to this mountain belt helps in reconstructing the orogenic evolution. Previous thermochronologic studies on the exhumation history of the western Alps using ^{40}Ar-^{39}Ar analyses of detrital white mica from the Tertiary Piemont basin (Carrapa et al., 2003) and from the Barrême basin (Morag et al., 2008) proposed a period of rapid exhumation of the western Alps at ca. 38–34 Ma. Given the wide range of potential closure temperatures of the ^{40}Ar-^{39}Ar system of 350–420 °C (e.g., von Blanckenburg et al., 1989), the dependence on the type of white mica (muscovite or phengite), and the size of the analyzed crystals (e.g., von Eynatten and Wijbrans, 2003), this method is less sensitive to upper-crustal exhumation processes than zircon fission-track (ZFT) and apatite fission-track (AFT) analyses. In addition, the findings of Morag et al. (2008) are based on a single blueschist pebble, which provided one young white mica ^{40}Ar-^{39}Ar age. Consequently, evidence exists for fast episodic exhumation in the western Alps between 38 and 34 Ma (Carrapa et al., 2003; Morag et al., 2008), but the transition to subsequent slower exhumation rates is poorly constrained for the western Alps. Additional fission-track analysis on detrital zircon from pro- and retro-side foreland basin deposits could provide more insight, but Malusà et al. (2011a) argued that zircons with 38–30 Ma cooling ages are in fact only derived from a volcanic source, rather than from bedrock exhumation in the western or central Alps. In order to address this question, we present new detrital AFT and ZFT data as well as zircon U/Pb analyses and single-grain ZFT-U/Pb double dating on key samples from Oligocene to early Miocene sedimentary rocks at Barrême (GSA Data Repository 1[1]), Montmaur, and Faucon du Caire from pro-side foreland basin remnants and from the Torino hills retro-side foreland basin (Fig. 1; GSA Data Repository 2 [see footnote 1]).

GEOLOGICAL SETTING

The western Alps are the result of convergence and collision between the Eurasian and the Apulian plates since 35 Ma (see Handy et al., 2010). The Penninic frontal thrust marks the limit between the internal and external western Alps (Fig. 1). From east to west, the internal western Alps consist of the high-pressure (HP), low-temperature (LT) metamorphic internal crystalline massif (Dora-Maira, Grand Paradiso, etc.), the Piemont Schistes lustrés complex, and the Briançonnais zone, bounded in

[1]GSA Data Repository Item 2013100, two geological maps, one of Barrême basin the second of Torino hills, is available at www.geosociety.org/pubs/ft2013.htm, or on request from editing@geosociety.org, Documents Secretary, GSA, P.O. Box 9140, Boulder, CO 80301-9140, USA.

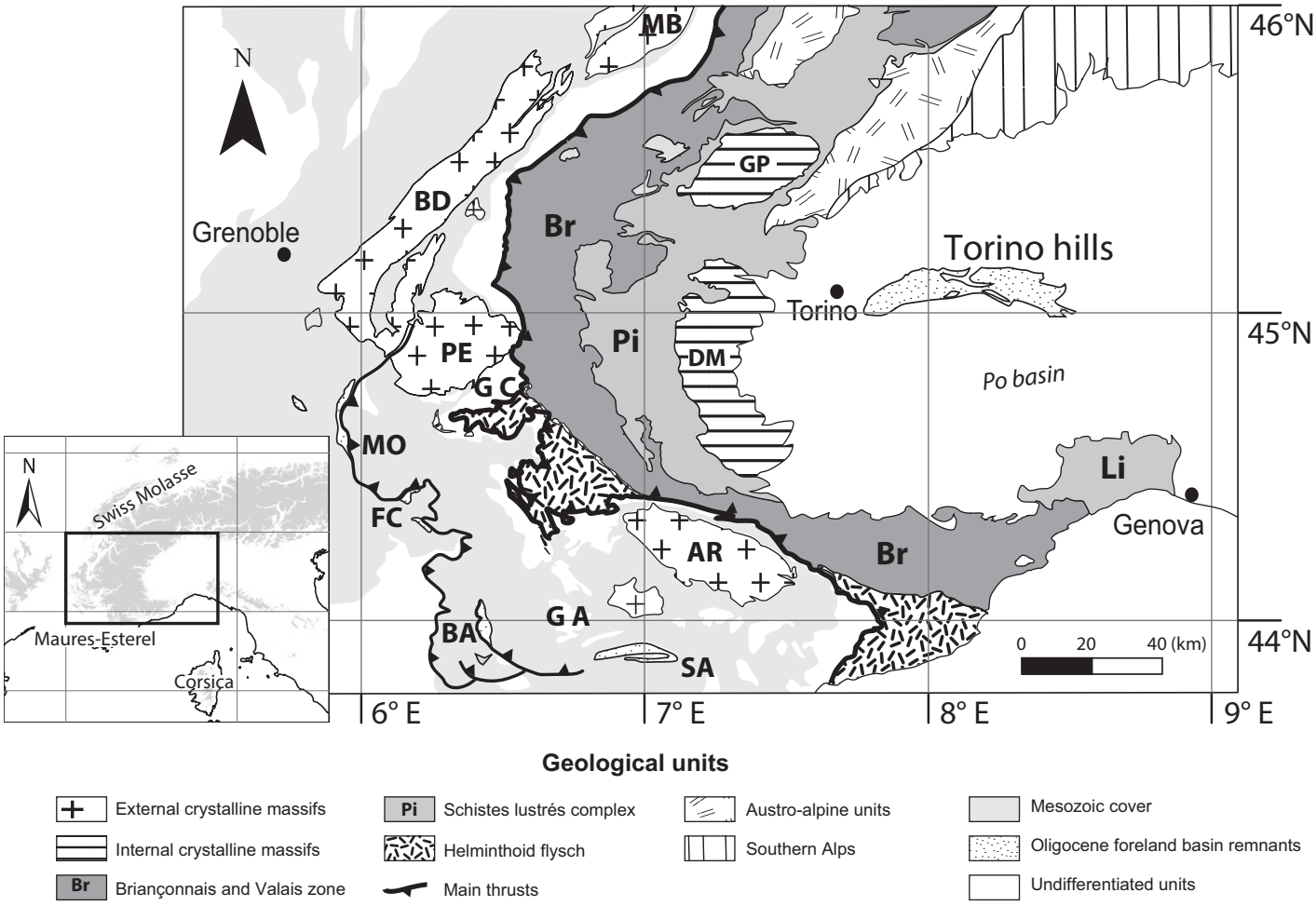

Figure 1. Overview map of the western Alps, showing the main lithotectonic units and the location of the foreland basin remnants used in this study. External massifs: MB—Mont Blanc, BD—Belledonne, PE—Pelvoux, AR—Argentera. Pro-side foreland basin remnants: MO—Montmaur, FC—Faucon du Caire, BA—Barrême basin, SA—Saint Antonin basin, GC—Grès du Champsaur, GA—Grès d'Annot. Internal massifs: GP—Gran Paradiso, DM—Dora-Maira. Other units: Li—Ligurian Alps.

the west by the nonmetamorphic Helminthoid flysch nappes (Fig. 1). The external western Alps are composed of the external crystalline massifs (Mont Blanc, Aiguilles Rouges, Pelvoux, Belledonne, and Argentera) and Permian–Triassic to Cretaceous sedimentary cover rocks of the former European passive margin. The external western Alps experienced only very low-grade Alpine metamorphism, but are nonmetamorphic for the most part (e.g., Schmid et al., 2004), and were deformed during Alpine shortening after the mid-Miocene (Schmid and Kissling, 2000; Graciansky et al., 2010).

Pro-Side Foreland Basin

Since the mid-Eocene, loading of the European lithosphere during convergence resulted in the formation of a flexural foreland basin to the west of the emerging mountain belt, as continental collision developed (Sinclair, 1997a). This development is marked by a marine transgression from the south and deposition of the shallow marine Calcaire à Nummulites limestone (see stratigraphic log in Fig. 2). Ford and Lickorish (2004) mapped this limestone unit to determine the advance of the marine transgression during continuous flexural subsidence from the Lutetian (41.4 Ma) to the Priabonian (33.7 Ma). The Calcaire à Nummulites is overlain by the Marnes Bleues (Fig. 2) and turbiditic sandstones such as the Grès de Champsaur or the Grès d'Annot in the deep (see map in Fig. 1), proximal part, and by the Grès de Ville in the distal part of the foreland basin (Sinclair, 1997b; Evans et al., 2004; Joseph and Lomas, 2004). At ca. 30 ± 1 Ma, the depositional environment in the pro-side foreland basin of the western Alps changed abruptly from marine to continental (Sinclair, 1997a), with deposition of conglomeratic units (e.g., the Conglomérat de Clumanc and Saint Lions in the Barrême basin; Figs. 1 and 2) and fluvial sandstones and mudstones in the distal part of the foreland basin, while the proximal part of the basin was deformed and integrated into the orogenic wedge. In the Swiss molasse basin, the transition between the lower marine to lower freshwater molasse occurred between 31 and 30 Ma, based on magnetostratigraphic calibration (Schlunegger et al., 1996; Kempf et al., 1999). Today, only remnants of the Eocene to early Miocene pro-side foreland basin deposits are preserved in southeastern France (Fig. 1), such as in the Barrême syncline (e.g., Evans et al., 2004), at Faucon du Caire (Gidon et al., 1991), and at Montmaur (Gidon, 1991). While the stratigraphy is well known for the Barrême basin (Callec, 2001), the depositional ages of the Montmaur and Faucon du Caire deposits are poorly constrained. The depositional age of the Montmaur conglomerate is estimated to be early Miocene (ca. 20 Ma; B. Pittet, 2012, personal commun.)

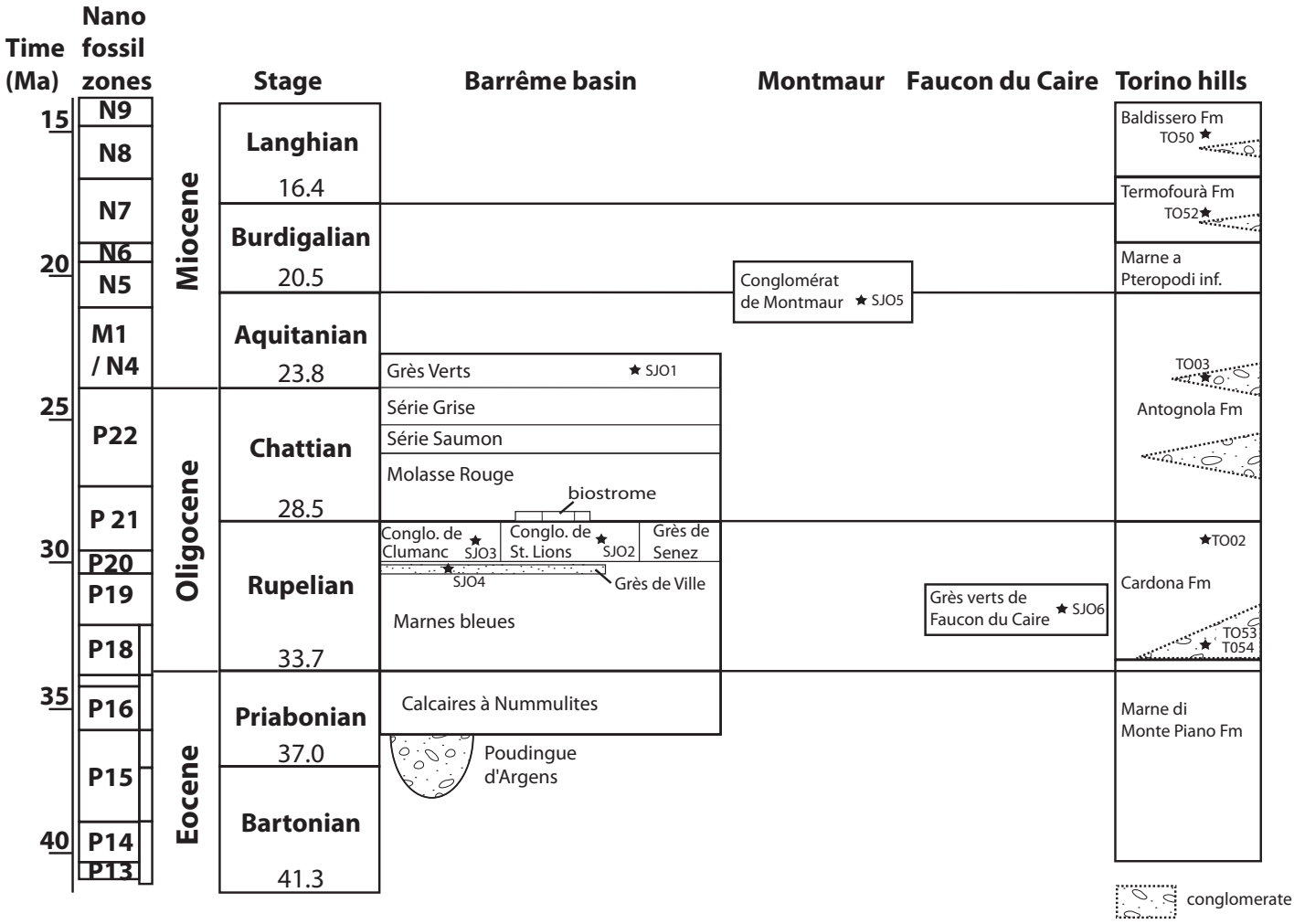

Figure 2. Stratigraphy of the Barrême basin, Montmaur, and Faucon du Caire basin in the pro-side foreland basin and the Torino hills in the retro-side foreland basin (after Callec, 2001; Festa et al., 2011). Biozone ages are from Berggren et al. (1995).

Andesitic volcanism in the western Alps has been dated with ^{40}Ar-^{39}Ar analyses at 36 to 31 Ma (Féraud et al., 1995; Montenat et al., 1999; Boyet et al., 2001). Andesitic pebbles and breccias can mainly be found in the Grès de Champsaur (Boyet et al., 2001) and the Saint Antonin basin (Bodelle, 1971), but also in the Conglomérat de Clumanc of the Barrême basin. After deposition of the first conglomerate units, the Barrême basin was filled with clastic continental deposits of the Molasse Rouge (Fig. 2). The youngest sedimentary rocks in this basin are the early Miocene Grès Verts, which are characterized by high serpentinite concentrations and were derived from the Piemont zone in the internal western Alps (Schwartz et al., 2012).

Retro-Side Foreland Basin

Subsidence in the retro-side foreland basin was caused by back-thrust loading during Oligocene to Miocene plate collision (Carrapa and Garcia-Castellanos, 2005), permitting deposition of the Tertiary Piemont basin sediments. A part of this foreland basin succession is exposed today in the west-plunging Torino hills anticline (Fig. 1; Mosca et al., 2007). The succession includes the Eocene marine Marne di Monte Piano Formation at the base, which is overlain by conglomerates and sandstones of the early Oligocene Cardona Formation and the late Oligocene to early Miocene Antognola Formation (Fig. 2). The overlying Marne a Pteropodi inferiori, and the sandy to conglomeratic Termofourà and Baldissero Formations are of middle Miocene depositional age (Festa et al., 2011; Fig. 2). While the Oligocene to early Miocene deposits of the southern Tertiary Piemont basin were mainly derived from the Ligurian Alps (Carrapa et al., 2004a, 2004b), the sediments preserved in the Torino hills have their source areas in the western Alps and the southern and central Alps to the north (Polino et al., 1991; Jourdan et al., 2013; Fig. 1), similar to the provenance of modern river sediments in the western Po basin drainage system today, as described by Garzanti et al. (2004) and Vezzoli et al. (2004).

METHODS

In total, 12 samples were analyzed for this study, six each from the pro- and retro-side foreland basins. The samples were collected from medium- to coarse-grained sandstones or from the sandy matrix of conglomerates, with the exception of sample TO53, for which diorite and granodiorite pebbles were collected. After rock crushing, all samples were sieved, and the 80–160 μm fraction was recovered. Apatite and zircon grains were separated using standard heavy liquid and magnetic separation techniques.

TABLE 1. DETRITAL APATITE FISSION-TRACK DATA OF THE BARRÊME BASIN AND MONTMAUR

Samples	Depositional age (Ma)	N	Age range (Ma)	P1 (Ma)	P2 (Ma)	P3 (Ma)	Central age (Ma)
Conglomérat de Montmaur SJ05	20.0 ± 4	110	12.0–188.9	21.7 ± 5.3 32.5%	45.9 ± 11.4 49.4%	97.5 ± 22.5 18.1%	43.6 ± 5.4
Grès Verts SJ01	23.0 ± 1	7	33.7–77.1	–	–	–	63.0 ± 15.9
Conglomérat de Saint Lions SJ02	29.0 ± 1	126	21.7–137.6	35.1 ± 9.0 5.2%	45.7 ± 19.2 29.5%	77.7 ± 17.2 19.3%	44.9 ± 8.3
Conglomérat de Clumanc SJ03	29.0 ± 1	95	19.9–135.5	36.8 ± 9.0 19.0%	59.2 ± 11.9 38.8%	91.7 ± 10.1 42.3%	65.9 ± 3.4
Grès de Ville SJ04	30.2 ± 1	36	22.3–135.3	–	43.7 ± 9.8 63.4%	88.9 ± 24.8 36.6%	56.0 ± 10.5

Note: N = total number of grains counted; binomial peak-fit ages are given ±2 standard error (SE). Also given is the percentage of grains in a specific peak. All samples were counted at 1250× dry (100× objective, 1.25 tube factor, 10 oculars) by S. Jourdan using a zeta (IRMM540R) of 214.63 ± 18.50 (1 SE) and by E. Hardwick using a zeta (IRMM540R) of 268.37 ± 7.61 (1 SE).

Fission-Track Dating

Apatite aliquots were mounted in epoxy resin, polished to expose internal grain surfaces, and etched with 5.5 mol HNO_3 for 21 s at 20 °C. The etched grain mounts were covered with muscovite sheets for external detector fission-track analysis. All samples were irradiated with a nominal fluence of 4.5×10^{15} n/cm^2 at the FRM II reactor at Garching, Germany, together with Fish Canyon Tuff and Durango Tuff age standards and IRMM540R uranium glass standards (15 ppm).

Zircon aliquots were mounted in Teflon® sheets, polished, and etched between 5 and 35 h in a NaOH-KOH eutectic melt at 228 °C. Two mounts were assembled per sample to allow etching for different lengths of time (e.g., Bernet et al., 2004a). The grain mounts were covered with muscovite sheets, and all samples were irradiated with a nominal fluence of 0.5×10^{15} n/cm^2 at the FRM II reactor at Garching, Germany, together with Fish Canyon Tuff and Buluk Tuff age standards and CN1 uranium glass standards (39.8 ppm).

After irradiation, the external mica detectors of all apatite and zircon samples were etched for 18 min in 48% HF at 21 °C to reveal induced tracks. All samples were counted dry at 1250× using an Olympus BX51 microscope and the FTStage 4.04 system of Trevor Dumitru.

The observed grain age distributions were decomposed into major grain-age components or peaks with binomial peak fitting using the BINOMFIT program of Brandon (Stewart and Brandon, 2004; Ehlers et al., 2005). However, individual peaks based on less than 20 grains per peak should be treated with caution, because they may not be fully representative (Vermeesch, 2004).

U/Pb and Single-Grain Zircon Fission-Track and U/Pb Double Dating

For U/Pb dating, zircon aliquots of two samples were mounted in epoxy resin for laser-ablation–inductively coupled plasma mass spectrometry (LA-ICP-MS) analyses at the Laboratoire Magmas et Volcans, Blaise Pascal University, Clermont-Ferrand, France. An Agilent 7500 ICP-MS and a fully computer-controlled 193 nm Resonetics M-50E excimer laser were used for ultrashort (<4 ns) impulsion spot analyses, with a 20-µm-diameter spot size (Paquette and Tiepolo, 2007; Tiepolo, 2003). The same technique was used for ZFT and U/Pb double dating. Zircons mounted in Teflon® sheets were first analyzed with the fission-track method and then dated with the U/Pb method. The objective was to analyze the core of the grains to determine if they had 30–38 Ma or much older (>>100 Ma) crystallization ages. We acknowledge that some zircons were affected by Pb loss, but that does not influence the objective of these analyses because no high-precision crystallization ages are needed to clearly distinguish 30–38 Ma versus much older (Hercynian or Pan-African) ages.

RESULTS

Fission-Track Results

Pro-Side Foreland Basin

The AFT data of five samples from the Barrême basin and Montmaur are shown in Table 1, and sample positions are given in Table 2. Sample SJ01 from the Grès Verts did not yield sufficient datable apatites to allow for peak fitting, as this lithology is very poor in heavy mineral content. Sample SJ02 (Conglomérat de Saint Lions), sample SJ03 (Conglomérat de Clumanc), and sample SJ04 (Grès de Ville) have very similar age ranges of ca. 20 Ma to 136 Ma, but they differ in peak ages, as sample SJ04 lacks the young peak at around 36 Ma (Table 1).

The ZFT data are presented in Table 3. All samples show wide age ranges with Miocene to Ordovician cooling ages. However, the main peak

TABLE 2. APATITE SAMPLE LOCATIONS

Samples	Latitude (°N)	Longitude (°E)
Grès Verts SJ01	43.943086	6.382749
Conglomérat de Saint Lions SJ02	43.983366	6.395649
Conglomérat de Clumanc SJ03	44.027245	6.384941
Grès de Ville SJ04	43.961917	6.376745
Conglomérat de Montmaur SJ05	44.506423	5.904279
Baldissero Formation TO50	45.073657	7.819
Termofourà Formation TO52	45.072202	7.816726
Antognola Formation TO03	45.066989	7.777501
Cardona Formation TO02	45.091323	7.795976
Cardona Formation TO53*	45.092596	7.813894
Cardona Formation TO54	45.093201	7.813593

*Selected diorite and granodiorite pebbles.

TABLE 3. DETRITAL ZIRCON FISSION-TRACK DATA OF THE BARRÊME BASIN, MONTMAUR, AND FAUCON DU CAIRE

Samples	Depositional age (Ma)	N	Age range (Ma)	P1 (Ma)	P2 (Ma)	P3 (Ma)
Conglomérat de Montmaur SJ05	20.0 ± 4	63	19.3–414.3	31.4 ± 10.4 11.0%	83.4 ± 26.7 43.8%	156.5 ± 49.5 45.2%
Grès Verts SJ01	23.0 ± 1	27	20.5–199.9	39.6 ± 10.2 45.6%	114.5 ± 35.3 54.4%	–
Conglomérat de Saint Lions SJ02	29.0 ± 1	161	13.8–454.9	30.1 ± 2.5 67.0%	62.6 ± 14.1 16.2%	186.8 ± 42.0 16.8%
Conglomérat de Clumanc SJ03	29.0 ± 1	28	14.5–284.8	30.1 ± 4.2 68.3%	123.7 ± 37.4 31.7%	–
Conglomérat de Clumanc SJ03 + 00MB55	29.0 ± 1	78	14.5–284.8	31.4 ± 3.5 53.8%	59.9 ± 17.5 13.1%	112.3 ± 20.1 33.2%
Grès de Ville SJ04	30.2 ± 1	61	32.5–427.6	48.2 ± 13.4 20.9%	101.6 ± 17.1 65.6%	232.5 ± 121.1 13.5%
Faucon du Caire SJ06	32.0 ± 5	52	31.7–319.4	47.3 ± 9.8 27.9%	139.0 ± 21.8 72.1%	–

Note: N = total number of grains counted; binomial peak-fit ages are given ±2 standard error (SE). Also given is the percentage of grains in a specific peak. All samples were counted at 1250× dry (100× objective, 1.25 tube factor, 10 oculars) by S. Jourdan using a zeta (CN1) of 104.39 ± 3.32 (1 SE). Data for sample 00MB55 are from Bernet et al. (2009). This sample was collected from the exact same layer in the outcrop location as sample SJ03.

age groups are late early Oligocene, Eocene, Cretaceous, and Jurassic. No indication of postdepositional resetting was found. In order to improve the data set for the Conglomérat de Clumanc, we added the 50 ZFT ages of sample 00MB55, published by Bernet et al. (2009), which was collected at the exact same spot in the outcrop location as sample SJ03 (Table 3). This allows the identification of three age components at ca. 31 Ma, 60 Ma, and 112 Ma.

Retro-Side Foreland Basin

AFT ages from the Torino hills are presented in Table 5, and samples position in Table 4. Samples TO54, TO53, and TO02 from the Cardona Formation have P1 peak ages between 29 Ma and 36 Ma and P2 peak ages between 50 Ma and 60 Ma. Only the sandstone samples TO02 and TO54 also contain a third peak P3 of 145 Ma and 94 Ma, respectively. The Antognola Formation sample TO03 contained too few datable grains to allow peak fitting, but it is remarkable that this sample displays the widest age range of all samples. The Termofourà Formation sample TO52 has peak ages at 31 Ma and 126 Ma, while the Baldissero Formation sample TO50 has two young peak ages at 23 Ma and 37 Ma. Therefore, all samples contain apatites with Alpine (<40 Ma) and older cooling ages (mainly Paleocene to Jurassic; Table 7).

The ZFT age peaks of the Torino hills samples are shown in Table 6. Only samples TO54 (Cardona Formation) and TO03 (Antognola Formation) have young age peaks with Alpine cooling ages, while basically all samples are dominated by zircons with pre-Alpine cooling ages.

Standard U/Pb and Single-Grain Fission-Track–U/Pb Double Dating

Zircon aliquots of two samples were analyzed with the U/Pb method only (see GSA Data Repository Tables DRT1 and DRT2 [see footnote 1]). Seventy-one randomly selected zircons of sample SJ03 of the Conglomérat de Clumanc in the Barrême basin show mainly Hercynian to Pan-African crystallization ages, and only three grains have an Oligocene Periadriatic volcanic crystallization age (Fig. 3A). The 85 zircons dated from the diorite and granodiorite pebbles of sample TO53 have almost exclusively Hercynian crystallization ages (Fig. 3B). Figure 3C shows the U/Pb results of volcanic zircons from the Barrême basin sediments, with a lower intercept at 32.9 ± 0.6 Ma.

In total, 133 single zircons from the Conglomérat de Clumanc (sample SJ03; 26 grains) and the Conglomérat de Saint Lions (sample SJ02, 107 grains) were analyzed with the double dating approach. The ZFT and U/Pb ages are shown in GSA Data Repository Tables DRT3 and DRT4 (see footnote 1). All data are plotted on a ZFT age versus U/Pb age diagram, shown in Figure 4A. In general, three ZFT-U/Pb age groups emerge. The first group contains the volcanic zircons with Oligocene U/Pb and ZFT ages. The second group has zircons with Oligocene ZFT ages and mainly Hercynian U/Pb ages, while the third group has a wide range of Cretaceous–Jurassic cooling ages and Hercynian or Pan-African U-Pb ages (Fig. 4A).

For the Torino hills, 97 zircons were double dated for three samples from the Cardona Formation (TO02, 46 grains), Antognola Formation (TO03, 18 grains), and the Termofourà Formation (TO52, 33 grains). In these

TABLE 4. ZIRCON SAMPLE LOCATIONS

Samples	Latitude (°N)	Longitude (°E)
Grès Verts SJ01	43.9595	6.40362
Conglomérat de Saint Lions SJ02	43.983382	6.395584
Conglomérat de Clumanc SJ03	44.027122	6.384963
Grès de Ville SJ04	44.044258	6.372468
Conglomérat de Montmaur SJ05	44.506392	5.904114
Faucon du Caire SJ06	44.391077	6.098306
Baldissero Formation TO50	45.073657	7.819
Termofourà Formation TO52	45.072202	7.816726
Antognola Formation TO03	45.066989	7.777501
Cardona Formation TO02	45.091323	7.795976
Cardona Formation TO53*	45.092596	7.813894
Cardona Formation TO54	45.093201	7.813593

*Selected diorite and granodiorite pebbles.

TABLE 5. DETRITAL APATITE FISSION-TRACK DATA OF THE TORINO HILLS

Samples	Depositional age (Ma)	N	Age range (Ma)	P1 (Ma)	P2 (Ma)	P3 (Ma)	Central age (Ma)
Baldissero Formation TO50	15.5 ± 1	24	15.8–72.2	22.8 ± 29.7 30.0%	36.5 ± 26.3 70.0%	–	31.3 ± 6.1
Termofourà Formation TO52	17.2 ± 1	53	17.3–401.7	31.1 ± 11.9 9.0%	126.2 ± 26.0 69.1%	–	49.3 ± 10.3
Antognola Formation TO03	23.5 ± 4	15	31.2–136.7	–	–	–	379.9 ± 72.5
Cardona Formation TO02	29.0 ± 5	67	15.8–186.4	29.0 ± 5.7 60.2%	53.3 ± 12.2 34.5%	145.2 ± 91.8 5.3%	38.0 ± 6.8
Cardona Formation TO53*	33.0 ± 5	102	14.3–79.6	31.8 ± 2.6 83.7%	50.9 ± 8.6 16.3%	–	34.5 ± 2.5
Cardona Formation TO54	33.0 ± 5	106	22.1–164.2	36.1 ± 3.9 52.1%	59.9 ± 13.9 31.9%	93.6 ± 19.4 16.0%	50.5 ± 2.6

Note: N = total number of grains counted; binomial peak-fit ages are given ±2 standard error (SE). Also given is the percentage of grains in a specific peak. All samples were counted at 1250× dry (100x objective, 1.25 tube factor, 10 oculars) by E. Hardwick using a zeta (IRMM540R) of 268.37 ± 7.61 (1 SE).
*Selected diorite and granodiorite pebbles.

TABLE 6. DETRITAL ZIRCON FISSION-TRACK DATA OF THE TORINO HILLS

Samples	Depositional age (Ma)	N	Age range (Ma)	P1 (Ma)	P2 (Ma)	P3 (Ma)
Termofourà Formation TO52	17.2 ± 1	36	31.3–414.7	47.2 ± 29.8 9.0%	126.2 ± 26.0 69.1%	232.1± 128.9 21.9%
Antognola Formation TO03	23.5 ± 4	26	18.4–216.1	25.5 ± 4.0 50.4%	101.5 ± 21.0 49.6%	–
Cardona Formation TO02	29.0 ± 4	119	48.1–620.9	77.7 ± 43.0 5.1%	140.0 ± 19.0 79.2%	271.6 ± 91.8 15.7%
Cardona Formation TO53*	33.0 ± 5	116	25.4–400.4	43.3 ± 17.2 6.2%	103.6 ± 29.3 47.8%	159.5 ± 37.1 46.0%
Cardona Formation TO54	33.0 ± 5	82	24.7–343.9	38.9 ± 11.1 5.6%	125.1 ± 24.4 65.9%	190.4 ± 87.1 28.5%

Note: N = total number of grains counted; binomial peak-fit ages are given ±2 standard error (SE). Also given is the percentage of grains in a specific peak. All samples were counted at 1250× dry (100× objective, 1.25 tube factor, 10 oculars) by S. Jourdan using a zeta (CN1) of 104.39 ± 3.32 (1 SE).
*Selected diorite and granodiorite pebbles.

TABLE 7. DETRITAL ZIRCON FISSION-TRACK DATA OF BARRÊME BASIN SAMPLES WITHOUT VOLCANIC GRAINS

Samples	Depositional age (Ma)	N	Age range (Ma)	P1 (Ma)	P2 (Ma)	P3 (Ma)
Conglomérat de Saint Lions SJ02	29.0 ± 1	133	17.6–460.9	30.0 ± 2.8 60.1%	60.2 ± 13.9 20.1%	189.7 ± 42.0 19.8%
Conglomérat de Clumanc SJ03	29.0 ± 1	26	14.5–284.8	31.5 ± 4.7 68.3%	137.2 ± 50.9 31.7%	–

Note: N = total number of grains counted; binomial peak-fit ages are given ±2 standard error (SE). Also given is the percentage of grains in a specific peak. All samples were counted at 1250× dry (100× objective, 1.25 tube factor, 10 oculars) by S. Jourdan using a zeta (CN1) of 104.39 ± 3.32 (1 SE). Because no grains from sample 00MB55 (see Table 3) were double dated, they could not be used for peak age calculations in this comparison.

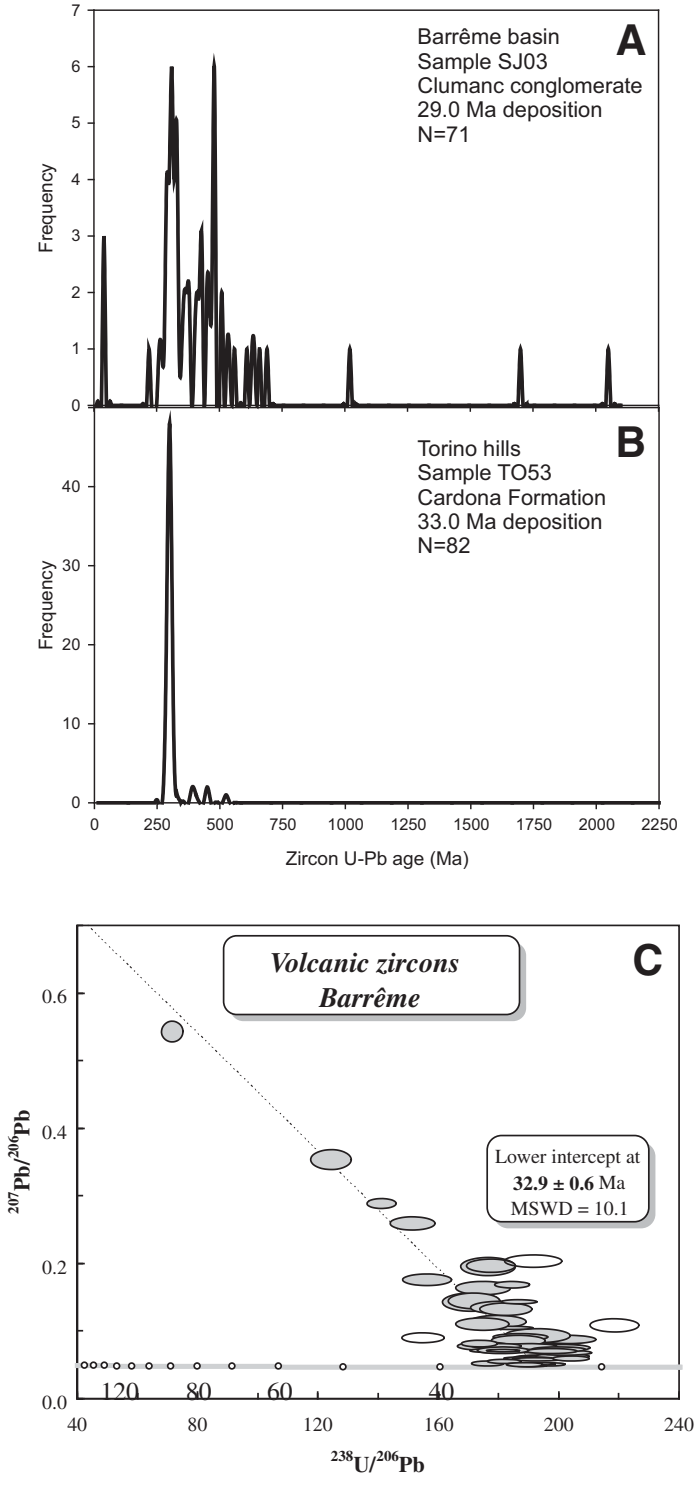

Figure 3. (A) Detrital zircon U/Pb data of the Conglomérat de Clumanc (sample SJ03) in the Barrême basin. (B) Zircon U/Pb ages of diorite and granodiorite pebbles from the Cardona Formation of the Torino hills anticline. (C) $^{238}U/^{206}Pb$ vs. $^{207}Pb/^{206}Pb$ diagram of zircons with volcanic origin from the Conglomérat de Clumanc and Conglomérat de Saint Lions in the Barrême basin. MSWD—mean square of weighted deviates.

samples, no zircons with Oligocene crystallization ages were observed, while ZFT ages ranged from the Oligocene to the Devonian (Fig. 4B).

By comparing the zircon U/Pb data of the Conglomérat de Clumanc from randomly selected grains with the data of double-dated grains, we see that the two populations are statistically identical (Fig. 5A), as they largely pass the Kolmogorov-Smirnov test (e.g., Press et al., 1992). This test is used to compare the age distributions of two samples, with a P(KS) probability value of <5% indicating that the difference is significant and systematic. If the P(KS) value is >>5%, the difference is most likely due to random chance alone. Given that the two aliquots of the Conglomérat de Clumanc sample showed the same age distribution, we combined them for comparison with the U/Pb data of the Conglomérat de Saint Lions sample. From Figure 5B, it is obvious that the Conglomérat de Saint Lions sample contains more volcanic zircons than the Conglomérat de Clumanc, even if these two conglomerates were deposited at the same time at a short distance from each other.

The fraction of volcanic grains, identified by double dating, can be subtracted from the original ZFT grain-age distributions of both samples of the Conglomérat de Saint Lions and Conglomérat de Clumanc (Table 3) in order to provide an unbiased signal of exhumation-related ZFT ages. The original and the "corrected" data sets for both samples show no significant difference (P[KS] = 72.7%; Fig. 6A), and the peak ages remain the same within error (Table 7; Fig. 6B).

DISCUSSION

Sediment Provenance

In order to determine sediment provenance, different types of information are available and need to be taken into account. Classical sandstone and conglomerate petrology provides the first line of evidence for sediment provenance. The pro-side foreland basin initially received most of its sediment from the south, as in the case of the Grès d'Annot (Sinclair, 1997b) or the Grès de Ville of the Barrême basin (Callec, 2001; Evans et al., 2004; Joseph and Lomas, 2004; see Fig. 1). Source areas were identified as the Maures-Estérel massif and Corsica on the basis of heavy mineral analyses (Evans and Mange-Rajetzky, 1991). From ca. 30 to 29 Ma on, basically all pro-side foreland basin sediments were derived from the western Alps (Evans and Mange-Rajetzky, 1991; Schwartz et al., 2012). This change in provenance is evident in the Conglomèrats de Saint Lions and Clumanc of the Barrême basin (Fig. 2), with deposition of so-called "exotic" pebbles such as gabbro, basalt, radiolarite, quartzite, and gneiss (Chauveau and Lemoine, 1961) derived from the internal western Alps at around 29 ± 1 Ma (Callec, 2001). Provenance information obtained for the Conglomérat de Clumanc and Conglomérat de Saint Lions from basalt pebble geochemistry (Jourdan et al., 2013) and Raman spectroscopy of detrital serpentinite (Schwartz et al., 2012) is consistent with this interpretation of an internal western Alps source.

Comparison of ZFT data of the Grès de Ville and the Conglomérat de Clumanc (Table 3) supports the hypothesis of a change in provenance at around 30 Ma of the proximal pro-side foreland basin sediments from a southern source to a dominant sediment source in the east to northeast, as the ZFT grain distributions of these two samples are significantly different (Fig. 7).

Interestingly, the youngest age peaks observed in the AFT data of the Conglomérat de Clumanc and Conglomérat de Saint Lions are somewhat older than the youngest age peaks observed in the ZFT data of the same samples (Tables 1 and 3), which could mean that the detrital apatites and zircons possibly did not come from exactly the same source rocks in the internal western Alps. This is not a surprise, as different source rock litholo-

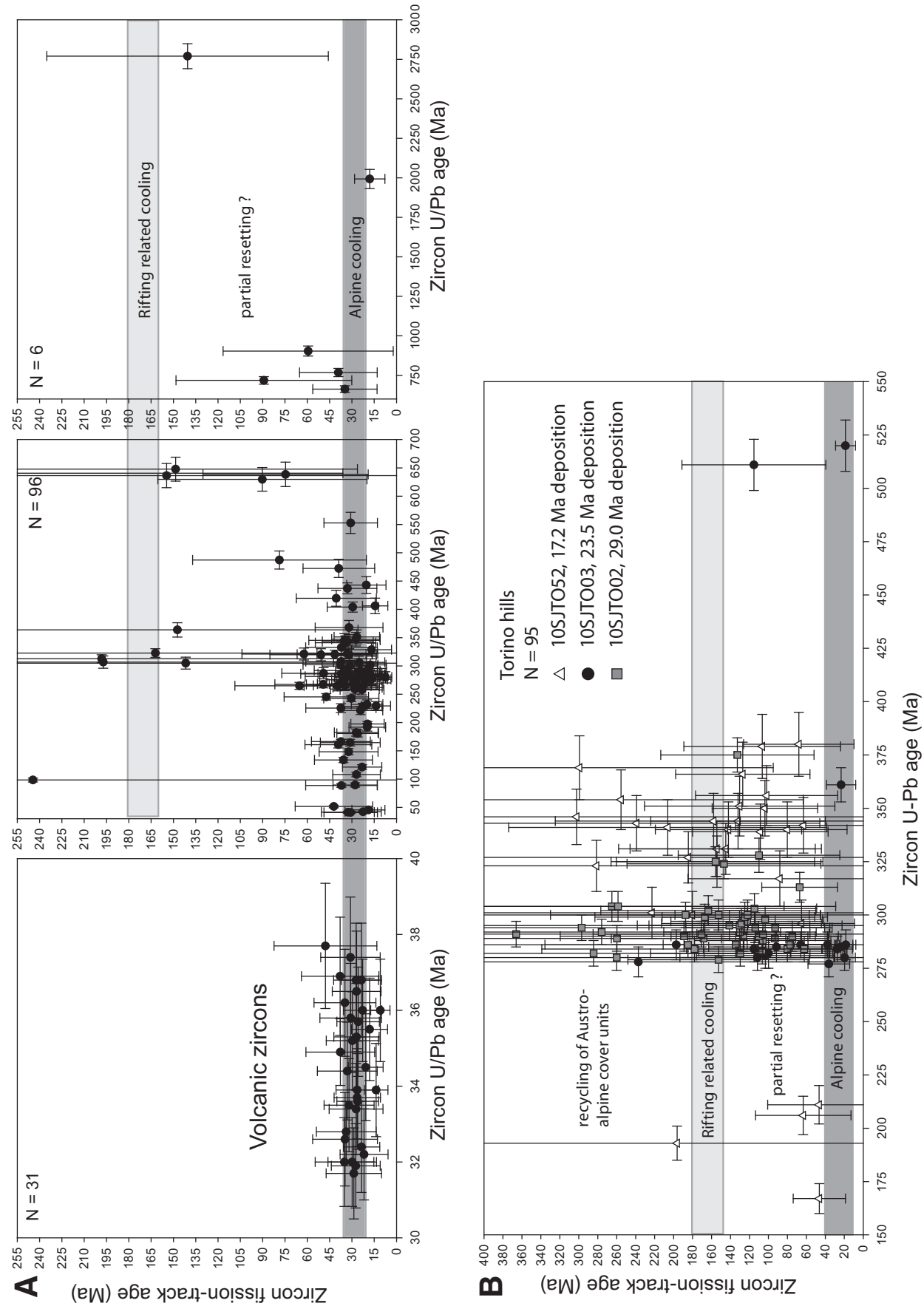

Figure 4. Single-zircon fission-track and U/Pb double-dating results. (A) The combined data of samples SJ02 (Conglomérat de Saint Lions) and SJ03 (Conglomérat de Clumanc) show three main zircon fission-track (ZFT)–U/Pb age groups. Group 1 consists of volcanic zircons with late Eocene–early Oligocene crystallization and cooling ages. Group 2 consists of zircons with Oligocene fission-track cooling ages and mainly Hercynian, but also Pan-African and older crystallization ages. Group 3 has Cretaceous–Jurassic ZFT cooling ages and Hercynian, Pan-African, or older crystallization ages. (B) Ninety-seven single ZFT–U/Pb double-dating results of three samples with different depositional ages. Zircons with Hercynian U/Pb show a wide spread of fission-track cooling ages, reflecting sediment derived from different levels of exhumation (non-reset sedimentary to zircons fully reset during alpine metamorphism).

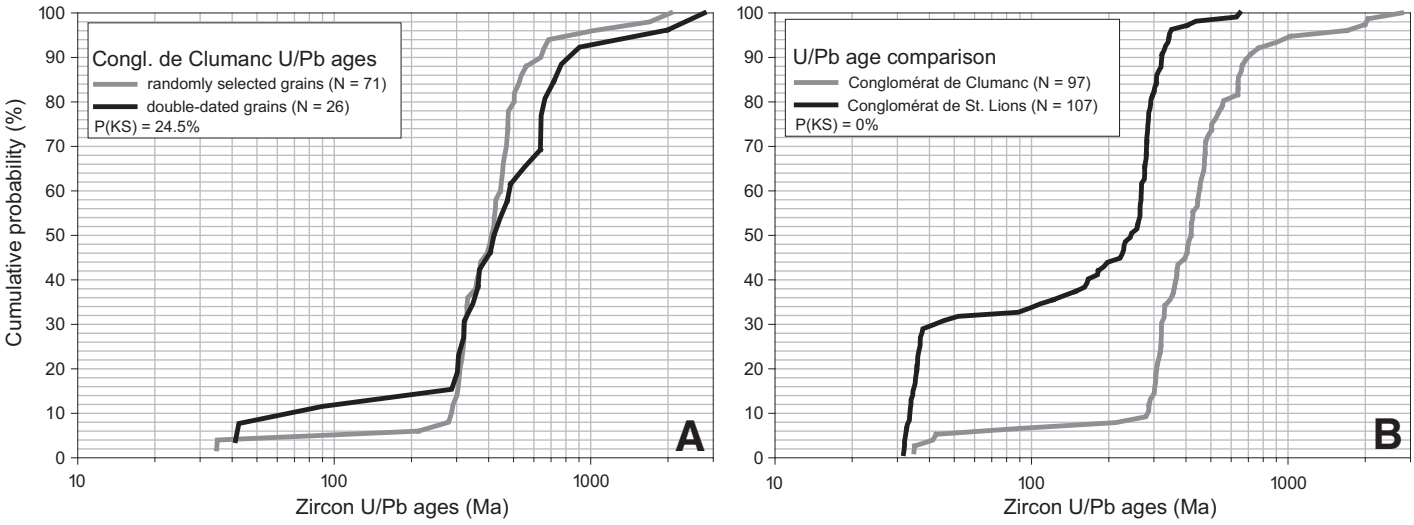

Figure 5. (A) Cumulative probability plots of the zircon U/Pb age distributions of two aliquots of sample SJ03 (Conglomérat de Clumanc). Zircons were dated with laser ablation–inductively coupled plasma–mass spectrometry (LA-ICP-MS) method. Grains were either randomly selected in aliquot 1 (gray curve), or double dated after fission-track analysis (black curve). The Kolmogorov-Smirnov (KS) statistics show that the two age distributions are not significantly different (see text). (B) Comparisons of zircon U/Pb age results of the Conglomérat de Saint Lions (SJ02) and the Conglomérat de Clumanc (SJ03). KS statistics indicate that the two age distributions are considerably different, as sample SJ02 contains more Oligocene volcanic zircons.

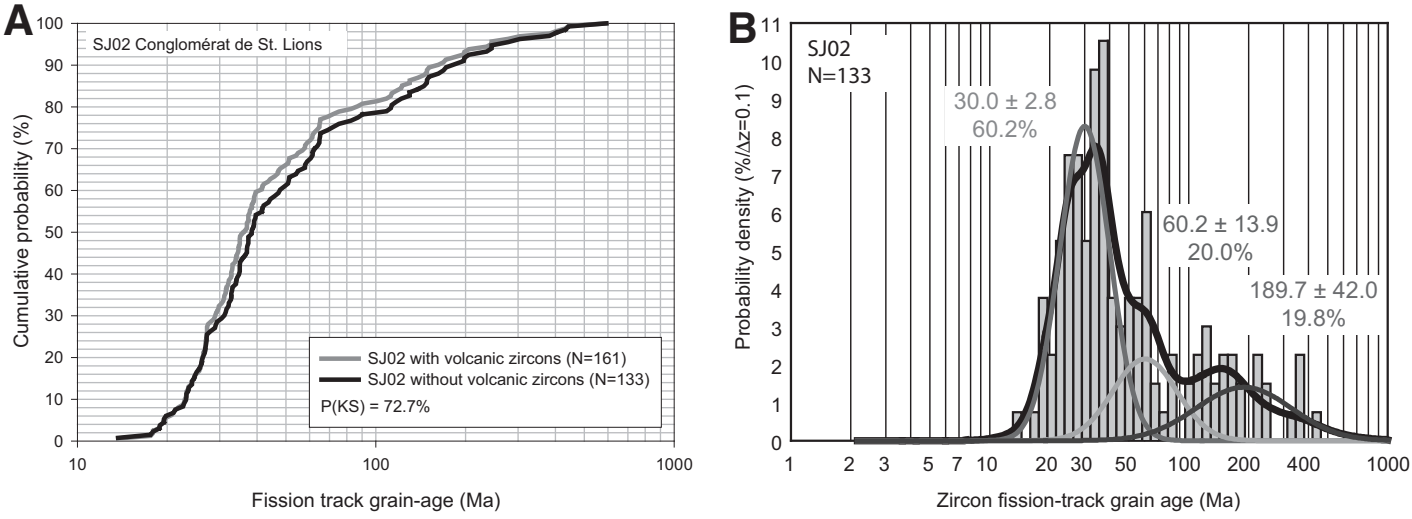

Figure 6. (A) Cumulative probability plot of the zircon fission-track (ZFT) results of sample SJ02. The gray curve shows the age distribution of all zircons analyzed with the method. The black curve shows the age distribution of the "corrected" data set, after removal of volcanic zircons, based on the double dating results. Kolmogorov-Smirnov (KS) statistics show that the two age distributions are basically identical and that the contribution of volcanic zircons does not perturb the exhumational signal. (B) Probability density plot of the "corrected" detrital ZFT grain-age distribution and best-fit peak ages of sample SJ02 from the Conglomérat de Saint Lions. Peaks were fitted with the BINOMFIT program (Stewart and Brandon, 2004; Ehlers et al., 2005).

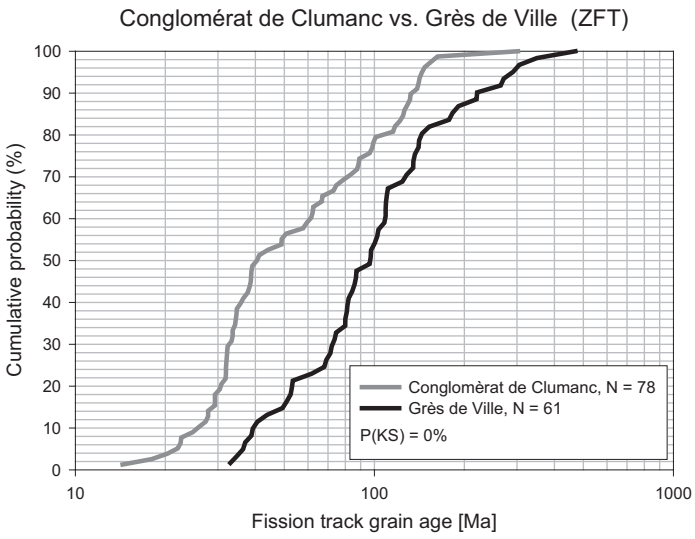

Figure 7. Cumulative probability plot to compare the zircon fission-track (ZFT) data of the Grès de Ville (SJ04) and the Conglomérat de Clumanc (SJO3). For this comparison, we combined the SJ03 ZFT data with published ZFT data of the Conglomérat de Clumanc (sample 00MB55) of Bernet et al. (2009), as the samples were collected at the same location. The Kolmogorov-Smirnov (KS) statistics of this comparison support the hypothesis of a change in provenance at around 30 Ma, as the ZFT grain distributions of the Conglomérat de Clumanc and the Grès de Ville are significantly different.

gies have variable apatite and zircon contents (e.g., Jakes and White, 1971, 1972; Deer et al., 1992). AFT–U/Pb double dating would be necessary to test if apatites with Oligocene cooling ages are of volcanic origin, but based on their mainly rounded grain shapes, this seems unlikely. The AFT age range observed in our samples is consistent with AFT bedrock data of rocks exposed in the internal western Alps today (see data compilations of Hunziker et al. [1992] or Vernon et al. [2008] and references therein).

The zircon U/Pb data indicate a contribution of Oligocene volcanic zircons (Figs. 3C and 4A) in the Conglomérat de Clumanc and Conglomérat de Saint Lions, and a few andesite pebbles have been observed in the field in these conglomerates. The source rocks of these volcanic zircons are not known. Heavy mineral analysis of an andesitic breccia in the Saint Antonin basin (Fig. 1), to the southeast of Barrême, showed that these rocks contain neither apatite nor zircon and have to be excluded as a potential source. This is consistent with the results of Boyet et al. (2001), who showed that andesitic melts in general in southern France experienced little continental contamination, and their zircon content is therefore very limited. For the zircons with Hercynian U/Pb ages, it is equally difficult to point to a precise source area in Oligocene times and to distinguish between southern sources (Maures-Estérel, Corsica, and Sardinia) or sources in the internal western Alps (Internal massifs, Austroalpine nappes, Briançonnais, etc.), as the Hercynian age signal is widespread in the Alps (e.g., Köppel, 1974; Paquette, 1987; Gebauer et al., 1992, 1997; Bussy et al., 1998; Bertrand et al., 2000, 2006; Dallagiovanna et al., 2009).

The Oligocene to Miocene sandstones and conglomerates in the Torino hills were essentially derived from the internal western Alps (Elter et al., 1966; Polino et al., 1991; Garzanti and Malusà, 2008; Festa et al., 2011; Jourdan et al., 2013), with possibly a minor contribution from the Ivrea zone of the southern Alps. The increase in the proportion of serpentinite and other ophiolite pebbles from the early to the late Oligocene (Polino et al., 1991) particularly demonstrates the increasing importance of the western Alps (e.g., Piemont zone) as a developing sediment source area. Hercynian zircon U/Pb ages obtained from diorite and granodiorite pebbles collected from the Cardona Formation (Fig. 3) hint at the internal crystalline massifs (e.g., Bertrand et al., 2006) or the Ivrea zone as potential sources. The Lepontine dome in the central Alps did not contribute sediment to the Torino hills, as these sediments were bypassed to the east to feed the Apennine foredeep (Dunkl et al., 2001; Garzanti and Malusà, 2008; Bernet et al., 2009).

Exhumation versus Volcanic Signal

The youngest ZFT age peaks determined from detrital samples collected around the Alps have been used in the past for estimating and tracking the rate of exhumation of the fastest-exhuming areas in the Alps over time (e.g., Spiegel et al., 2000, 2001; Bernet et al., 2001, 2009; Carrapa, 2009; Bernet, 2010). For example, simple first-order exhumation rates can be estimated using a one-dimensional (1-D) thermal advection model calculated with the "Age2Edot" program of M. Brandon (for details, see Ehlers et al., 2005). For a given set of parameters (e.g., thermal gradient, internal heat production, thermal diffusivity, geothermal gradient, and surface temperature), a relationship between the lag time of a given peak age and an exhumation rate is determined (Fig. 8A). Lag time is defined as the difference between the cooling age or peak age and the time of deposition of the sediment (e.g., Garver et al., 1999). In the absence of postdepositional thermal resetting, the rule of thumb is the shorter the lag time, the faster is the estimated exhumation rate. We acknowledge that this approach has considerable limitations because it is more suitable for steady-state conditions than for episodic exhumation, but to keep consistency and comparability with exhumation rate estimates in previous studies (e.g., Bernet et al., 2001, 2009; Bernet and Tricart, 2011), we decided to follow this approach. We estimate that the exhumation rates of the fastest-exhuming area in the internal western Alps during the late early Oligocene were at least on the order of 1.5–2 km/m.y., which should be regarded as a relatively conservative first-order estimate only, given the detection limits of this approach for very short lag times (<1–2 m.y.), as shown in Figure 8A.

Despite the importance of tectonic extension with respect to exhumation of high-pressure and ultrahigh-pressure rocks in the western Alps (Rubatto and Hermann, 2001; Sue and Tricart, 2002, 2003; Schwartz et al., 2009), upper-crustal near-surface (6–8 km depth) exhumation was probably driven mainly by erosion (e.g., Evans and Mange-Rajetzky, 1991; Garzanti et al., 2004; Morag et al., 2008; Bernet and Tricart, 2011). The lack of large volumes of sediment deposited at that time is used as an argument against fast erosional exhumation (Malusà et al., 2011a). It is possible that the fast erosional exhumation may have affected only a small area in the beginning and did not produce large amounts of sediment, but it is known that at around 30 Ma, the depositional environment abruptly changed from marine to continental with a switch from an underfilled to an overfilled pro-side foreland basin (Sinclair, 1997a, 1997b). The volume of late Oligocene sediments deposited in the pro-side foreland basin is very poorly known (see estimates by Kuhlemann, 2000), because of removal during late Miocene recycling of foreland basin sediments.

Malusà et al. (2011a) argued that the young age peaks observed in the detrital ZFT data sets do not consist of zircons derived from exhumation of metamorphic rocks in the western and central Alps, but are only derived from Periadriatic magmatic rocks. This argument may hold true for the volcaniclastic Gonfolite rocks in the direct vicinity of the Bergell intrusion complex (Malusà et al., 2011a), but our double-dating results show that this is not correct for the western Alps. While single-grain ZFT and U/Pb double dating confirm the presence of Oligocene volcanic zircons,

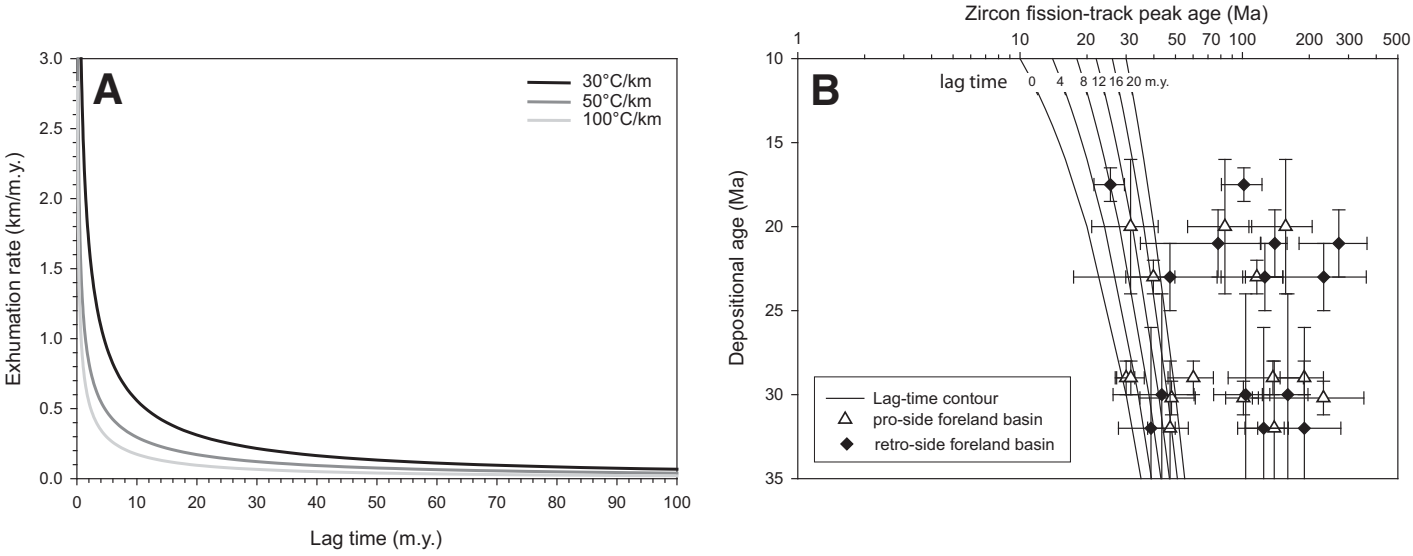

Figure 8. (A) Lag time versus exhumation rate plot. The lag time and exhumation rate relationship for radiation-damaged zircon was calculated for three different thermal gradients with the Age2Edot program of Brandon, as described in Ehlers et al. (2005). The thermal model parameters are: Layer depth to constant temperature (ZLW) 30 km, thermal diffusivity (kappa) 19.19 km²/m.y., internal heat production 8 °C/m.y., surface temperature 10 °C, temperature at base of layer (Tlw) 910 °C, surface thermal gradients of 30 °C/km, 50 °C/km, and 100 °C/km, estimated volumetric heat production 0.752909 μW/m³, estimate for thermal conductivity 2.823409 W/(m/K), and surface heat flux 84.70226 mW/m²; estimates assume density and thermal conductivity are 2700 kg/m³ and 1100 J/kg²K, respectively. For radiation-damaged zircon, the default fission-track annealing parameters are: activation energy for 50% annealing 49.8 kcal/mole, annealing parameter beta 3.16 × 10^{-22} /m.y. (B) Lag-time plot of detrital zircon fission-track (ZFT) grain-age peaks of the pro- and retro-side foreland basin samples of this study. All samples contain several age peaks, but only the youngest peak (P1) in each sample is used for estimating the exhumation rates of the fastest-exhuming areas.

these zircons can be identified and eliminated from the ZFT data set. As shown in Figure 6A and Table 7, it becomes obvious that the signal of relatively fast exhumation is persistent. The contribution of volcanic zircon is insignificant in this respect, probably because the volume of magmatic material generated in the Alps during the early Oligocene is rather limited and only of local importance. Today, Periadriatic rocks cropping out in the Alps make up only a very small percentage (<5%) of the surface area of the Alps.

For the double-dated samples analyzed from the Torino hills, no zircons with Oligocene crystallization ages were observed. Therefore, all ZFT ages reflect bedrock exhumation in these samples. Overall, the Torino hills ZFT ages are older than the ZFT ages determined in the pro-side foreland basin sediments, reflecting mainly removal of non-reset or only partially reset cover units in the eastern part of the internal western Alps. In addition, the Oligocene and Cretaceous detrital muscovite ^{40}Ar-^{39}Ar ages of Carrapa et al. (2003) in the Tertiary Piemont basin and of Morag et al. (2008) from the Barrême basin also support the argument of erosion of cover units and crystalline basement.

Unfortunately, the Oligocene depositional ages in the Torino hills stratigraphy are not very precisely known, and that is why we did not estimate exhumation rates for the samples collected in the retro-side foreland basin. The youngest AFT age peak observed in the Cardona and Termofourà Formations of ca. 30 Ma (Table 3) is younger than the AFT age peaks observed in the pro-side foreland basin sediments. The ZFT signal, on the other hand, is in general much older than in the pro-side foreland basin, with the exception of sample TO03 of the Antognola Formation. Therefore, the fast exhumation signal in the retro-side basin is better preserved in the AFT data of this study and the muscovite ^{40}Ar-^{39}Ar data of Carrapa et al. (2003).

Fast rates of erosion are linked to local relief in certain mountain belts (Montgomery and Brandon, 2002). Local relief in the late Oligocene western Alps may have only been on the order of 1–1.5 km, with means topographic elevations of 2–3 km, similar to the central Alps at that time, as speculated by Pfiffner (1986), Schlunegger et al. (1996, 1997), Kempf et al. (1999), Spiegel et al. (2000, 2001), Kühni and Pfiffner (2001), or Schlunegger and Simpson (2002). However, only Campani et al. (2012) provided concrete evidence for the existence of high (similar to present day) topography and relief in the central Alps at least since the mid-Miocene, based on isotopic analyses. The occurrences of large serpentinite blocks and olistoliths deposited during the Oligocene in the retro-side foreland basin provide the petrologic evidence of erosion of the internal western Alps. This suggests the existence of steep slopes on the eastern flank of the orogen, from where this debris was derived, hinting at significant relief.

The phase of fast erosion in the western Alps was short-lived, probably lasting only 2–3 m.y. (Fig. 8B). Erosion rates slowed down to 0.2–0.3 km/m.y. during the late Oligocene, comparable to what can be discerned from detrital AFT and ZFT data of Miocene sandstone and present-day river sediments on the pro-side (Fig. 8B; Bernet et al., 2004a, 2004b, 2009; Glotzbach et al., 2011) or thermochronologic and sediment petrologic data from the retro-side (e.g., Carrapa et al., 2003, 2004a; Garzanti et al., 2004; Vezzoli et al., 2004).

Geodynamic Framework

Three main scenarios have been proposed to identify the underlying tectonic driving force for the development of the western Alps. First, Sinclair (1997a) suggested that the change from flysch to molasse deposition and a large increase in the sediment deposition in the foreland basin were driven by rapid isostatic surface uplift of the orogen caused by slab breakoff, better constrained in the northern western Alps and the central Alps, between 35 and 30 Ma (von Blanckenburg and Davies, 1995; Handy et al.,

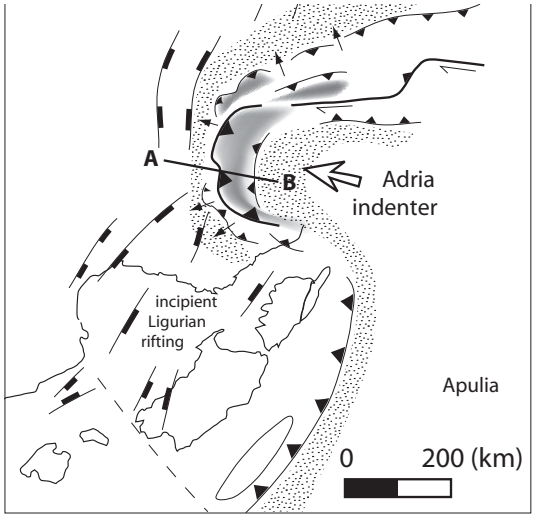

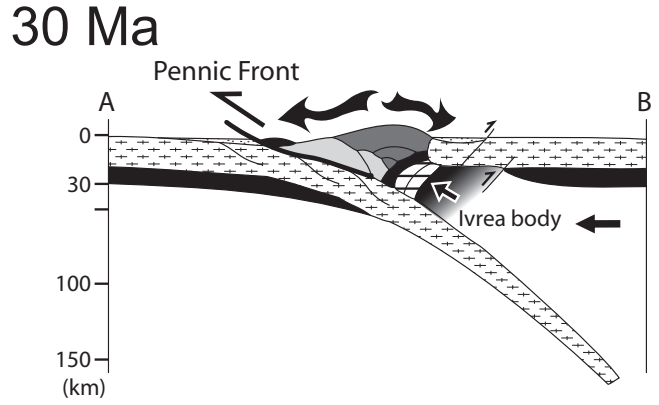

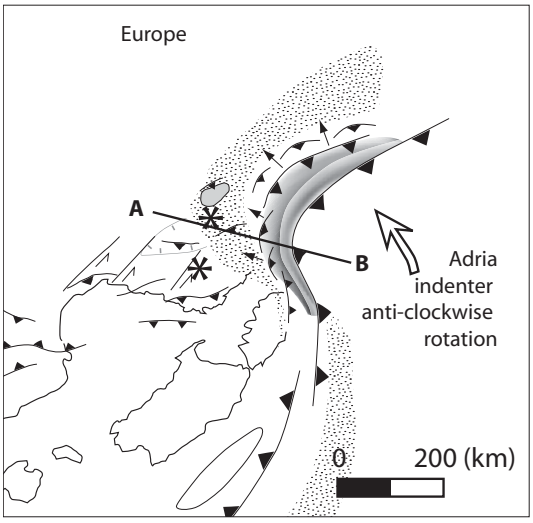

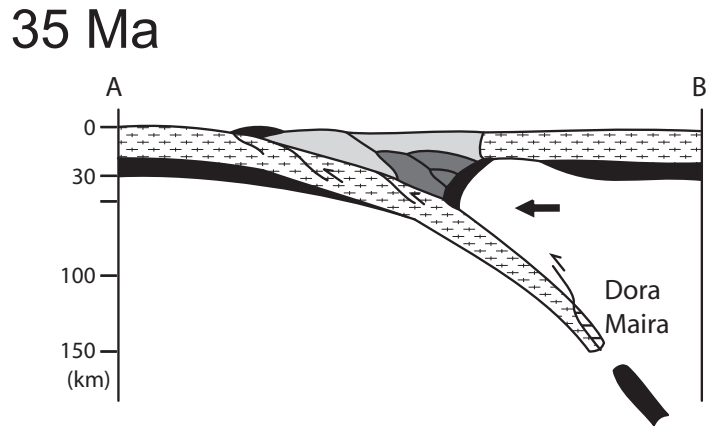

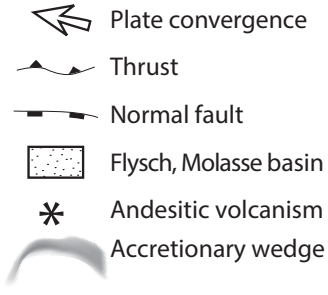

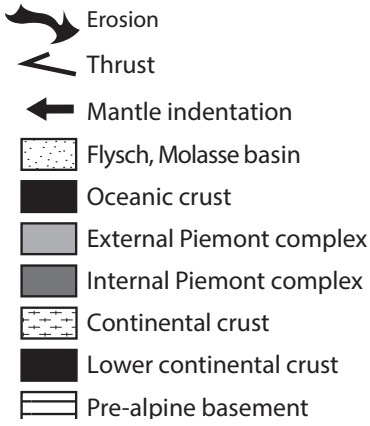

Figure 9. Paleogeographic map and cross section of the western Alps with the plate-tectonic situation at ca. 35–30 Ma (after Schmid and Kissling, 2000; Handy et al., 2010; Dumont et al., 2012). Continental collision started at ca. 35 Ma, followed by intermediate-depth slab breakoff and subsequent surface uplift and Ivrea body emplacement.

2010). Second, geophysical analyses of the deep structure of the western Alps showed the presence of the Ivrea body in the core of the orogenic arc, at less than 8 km depth (Schmid and Kissling, 2000; Schwartz, 2000; Paul et al., 2001; Lardeaux et al., 2006). The Ivrea body, which is interpreted as a sliver of the Apulian plate (Lardeaux et al., 2006), is acting as a vertical indenter against the European plate during east-west convergence (Handy et al., 2010). This indenter may have supported surface uplift in the western Alps contemporaneous with emplacement of nappes and development of the flower structure of the internal western Alps during continental collision (Tricart and Sue, 2006; Tricart and Schwartz, 2006). Finally, Malusà et al. (2011b) proposed that by late Eocene to early Oligocene times, NNE-directed motion of the Apulian plate induced localized extension within the southern part of the Alpine belt, and allowed tectonic and fast emplacement of eclogitic units without erosion. If this model accounts for the exhumation of southern eclogitic massifs (Erro Tobio, Corsica), it cannot explain the later exhumation of the Monviso ophiolitic massif, as fission-track data and detrital records in the Torino hills show that by early Oligocene times, this massif was still at a depth of ~10 km and was at the surface during the early late Oligocene (Schwartz et al., 2009, 2012).

Numerical modeling of slab breakoff, lithosphere dynamics, and topographic response by Duretz et al. (2011) provides a theoretical framework for linking slab breakoff and the topographic evolution of the western Alps, as the scenarios presented previously can be combined. Currently, the subducted European slab is at ~300 km depth beneath the western Alps (Piromallo and Faccenna, 2004). Plate-tectonic reconstructions by Schmid and Kissling (2000) and Handy et al. (2010) suggest that the European slab was initially longer, and breakoff between 35 and 30 Ma occurred at a depth of ~150–200 km. The "intermediate-depth (150–200 km) slab breakoff" model of Duretz et al. (2011) allows explanation of the topographic evolution of the western Alps. Duretz et al. (2011) stated that intermediate slab breakoff at the oceanic-continental crust transition causes surface uplift of the overriding plate at a rate of 0.5 km/m.y. by isostatic rebound after ~1 m.y. Slab breakoff, followed by surface uplift, is synchronous with counterclockwise rotation of the Apulian plate, a change in the convergence direction from south-north to east-west between the Apulian and Eurasian plates, and crustal thickening during continent-continent collision, which started at ca. 35–30 Ma (Handy et al., 2010; Malusà et al., 2011b; Dumont et al., 2012). This global and brutal kinematic change is linked with slab retreat in the nascent Mediterranean realm, inducing a strong westward mantle flow beneath the southern western Alps (Jolivet et al., 2009), following the two-subduction zone model of Handy et al. (2010). Pfiffner et al. (2002) considered that the Ivrea body was involved in the Alpine orogeny by 30 Ma in the northeastern Alps, but it did not affect the western Alps until ca. 15 Ma. In the southern part of the Alps, the counterclockwise rotation of the Apulian plate induced extension by early Oligocene times (Malusà et al., 2011b). In the western Alps, the Apulian plate indented the internal zone (Dumont et al., 2012), creating a high topography (Schwartz et al., 2012). Thus, we proposed that the Ivrea body, corresponding to the edge of the Adriatic mantle, indented the internal zone and sustained the high topography created by around 30–29 Ma (Figs. 9 and 10).

In the central and southern Alps, Oligocene Periadriatic magmatism on the overriding plate, for example, at Biella or Bergell, is seen in relation to slab breakoff (von Blanckenburg and Davies, 1995; Piromallo and Faccenna, 2004). In the southern western Alps, the situation is different. The brief phase of andesitic volcanism in the external Alps between 36 and 31 Ma, with its main activity at around 32 Ma (e.g., Féraud et al., 1995; Boyet et al., 2001), occurred very locally on the subducting European plate, only along the southern edge of the Pelvoux massif and in the Saint Antonin area (Fig. 1). This volcanism cannot be explained by slab breakoff of the European slab at 35 Ma, as it affects the pro-side foreland basin and not the internal zone, but seems more likely to be related to flow and upwelling of hot mantle material beneath the European plate in relation to slab rollback of the nearby Apennine (or Ligurian) slab to the east at that time (Garzanti and Malusà, 2008; Vignaroli et al., 2008; Jolivet et al., 2009; Handy et al., 2010). Magma-crust interaction is characteristic for this kind of magmatism (e.g., Wilson, 1989). The Oligocene andesitic volcanic rocks of the western Alps show moderate continental contamination with depletion in Nb and Ta, and they have less of a continental signature than the acidic rocks of the Bergell massif for example (Boyet et al., 2001).

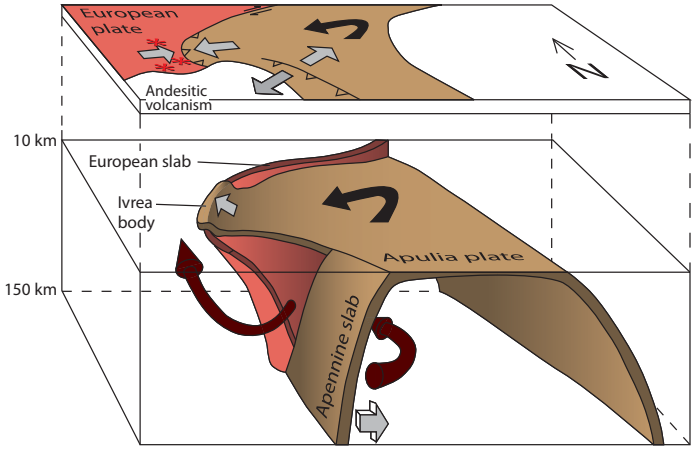

Figure 10. Three-dimensional (3-D) block diagram showing the slab geometry of the Apulian and European plates between 35 and 30 Ma (modified from Vignaroli et al., 2008). Counterclockwise rotation of the Apulian plate generated extension in the southern part of the Alps, an Apennine-Alps transition zone, and convergence in the western Alps. The Ivrea body was emplaced during this phase in the western Alps. Slab rollback of the Apennine slab generated a toroidal mantle flow, causing upwelling of hot mantle material beneath the European plate (Vignaroli et al., 2008), which triggered limited local andesitic volcanism.

CONCLUSIONS

The Oligocene is a key period in the evolution of the western Alps during continental collision. Underlying plate-tectonic processes, including a change in convergence direction, intermediate-depth slab breakoff of the European slab, and indentation of the Ivrea body caused surface uplift. This period is marked by short phase of fast exhumation, as well as changes in subsidence and basin fill of the pro- and retro-side foreland basins. Fast exhumation of at least 1.5–2 km/m.y., estimated from detrital zircon ZFT and U/Pb double dating of single grains of mid-Oligocene sedimentary rocks of the pro-side foreland basin, reflects a critical period during the evolution of the mountain belt. Despite the occurrence of contemporaneous volcanism, the exhumation signal is persistent and clearly recognizable in the geothermochronologic data. During the late Oligocene, erosion rates slowed down to ~0.2 km/m.y. on average, similar to present-day erosion rates in the western Alps. The brief episode of early Oligocene andesitic volcanism on the subducting European plate is seen as a result of slab retreat of the Apennine slab and upwelling of hot upper mantle, and not related to slab breakoff of the European slab.

ACKNOWLEDGMENTS

We gratefully acknowledge constructive and insightful reviews by Fritz Schlunegger, an anonymous reviewer, and Editor Eric Kirby, which helped us to improve this manuscript. Financial support for this research was provided by an Agence National de la Recherche–Erosion and

Relief Development in the Western Alps grant. We thank Francois Senebier, Francis Coeur, and Vincent Bouvier for help with sample preparation.

REFERENCES CITED

Berggren, W.A., Hilgen, F.J., Langereis, C.G., Kent, D.V., Obradovich, J.D., Raffi, I., Raymo, M.E., and Shackleton, N.J., 1995, Late Neogene chronology—New perspectives in high-resolution stratigraphy: Geological Society of America Bulletin, v. 107, p. 1272–1287, doi:10.1130/0016-7606(1995)107<1272:LNCNPI>2.3.CO;2.

Bernet, M., 2010, Tracing exhumation and orogenic wedge dynamics in the European Alps with detrital thermochronology—Comment: Geology, v. 38, p. e226, doi:10.1130/G31173C.1.

Bernet, M., and Tricart, P., 2011, The Oligocene orogenic pulse in the southern Penninic arc (western Alps): Structural, sedimentary and thermochronological constraints: Bulletin de la Societe Geologique De France, v. 182, no. 1, p. 25–36.

Bernet, M., Zattin, M., Garver, J.I., Brandon, M.T., and Vance, J.A., 2001, Steady-state exhumation of the European Alps: Geology, v. 29, p. 35–38, doi:10.1130/0091-7613(2001)029<0035:SSEOTE>2.0.CO;2.

Bernet, M., Brandon, M.T., Garver, J.I., and Molitor, B., 2004a, Fundamentals of detrital zircon fission-track analysis for provenance and exhumation studies, *in* Bernet, M., and Spiegel, C., eds., Detrital Thermochronology—Provenance Analysis, Exhumation, and Landscape Evolution of Mountain Belts: Geological Society of America Special Paper 378, p. 25–36.

Bernet, M., Brandon, M.T., Garver, J.I., and Molitor, B., 2004b, Downstream changes of Alpine zircon fission-track ages in the Rhône and Rhine Rivers: Journal of Sedimentary Research, v. 74, p. 82–94, doi:10.1306/041003740082.

Bernet, M., Brandon, M., Garver, J., Balestieri, M.L., Ventura, B., and Zattin, M., 2009, Exhuming the Alps through time: Clues from detrital zircon fission-track thermochronology: Basin Research, v. 21, p. 781–798, doi:10.1111/j.1365-2117.2009.00400.x.

Bertrand, J.M., Pidgeon, R.T., Leterrier, J., Guillot, F., Gasquet, D., and Gattiglios, M., 2000, SHRIMP and IDTIMS U-Pb zircon ages of the pre-Alpine basement in the Internal Western Alps (Savoy and Piemont): Schweizerische Mineralogische und Petrographische Mitteilungen, v. 80, p. 225–248.

Bertrand, J.M., Paquette, J.L., and Guillot, F., 2006, Permian zircon U-Pb ages in the Gran Paradiso massif: Revisiting post-Variscan events in the western Alps: Schweizerische Mineralogische und Petrographische Mitteilungen, v. 85, p. 15–29.

Bodelle, J., 1971, Les Formations Nummulitiques de l'Arc de Castellane [Thèse d'Etat]: Nice, France, Université de Nice, A5041.

Boyet, M., Lapierre, H., Tardy, M., Bosch, D., and Maury, R., 2001, Sources of the andesitic components in the Taveyannaz Sandstones and Champsaur Sandstones: Implications for the Paleogene geodynamic evolution of the Alps: Bulletin de la Société Géologique de France, v. 172, p. 487–501, doi:10.2113/172.4.487.

Bussy, F., Venturini, G., Hunziker, J., and Martinotti, G., 1998, U-Pb ages of magmatic rocks of the western Austroalpine Dent Blanche–Sesia Unit: Schweizerische Mineralogische und Petrographische Mitteilungen, v. 78, p. 163–168.

Callec, Y., 2001, La Déformation Synsédimentaire des Bassins Paléogènes de l'Arc de Castellane (Annot, Barrême, St-Antonin) [Ph.D. thesis]: Paris, France, Ecole des Mines de Paris.

Campani, M., Mulch, A., Kempf, O., Schlunegger, F., and Mancktelow, N., 2012, Miocene paleotopography of the central Alps: Earth and Planetary Science Letters, v. 337–338, p. 174–185, doi:10.1016/j.epsl.2012.05.017.

Carrapa, B., 2009, Tracing exhumation and orogenic wedge dynamics in the European Alps with detrital thermochronology: Geology, v. 37, p. 1127–1130, doi:10.1130/G30065A.1.

Carrapa, B., and Garcia-Castellanos, D., 2005, Western Alpine back-thrusting as subsidence mechanism in the Tertiary Piedmont basin (western Po Plain, NW Italy): Tectonophysics, v. 406, p. 197–212, doi:10.1016/j.tecto.2005.05.021.

Carrapa, B., Wijbrans, J., and Bertotti, G., 2003, Episodic exhumation in the western Alps: Geology, v. 31, p. 601–604, doi:10.1130/0091-7613(2003)031<0601:EEITWA>2.0.CO;2.

Carrapa, B., Wijbrans, J., and Bertotti, G., 2004a, Detecting provenance variations and cooling patterns within the western Alpine orogen through $^{40}Ar/^{39}Ar$ geochronology on detrital sediments; the Tertiary Piedmont basin, northwest Italy, *in* Bernet, M., and Spiegel, C., eds., Detrital Thermochronology—Provenance Analysis, Exhumation, and Landscape Evolution of Mountain Belts: Geological Society of America Special Paper 378, p. 67–103.

Carrapa, B., Di Giulio, A., and Wijbrans, J., 2004b, The early stages of the Alpine collision: An image derived from the Upper Eocene–Lower Oligocene record in the Alps–Apennines junction area: Sedimentary Geology, v. 171, p. 181–203, doi:10.1016/j.sedgeo.2004.05.015.

Chauveau, J.C., and Lemoine, M., 1961, Contribution à l'étude géologique du synclinal tertiaire de Barrême (moitié nord): Bulletin de la Carte Géologique de France, v. 264, p. 147–178.

Dallagiovanna, G., Gaggero, L., Maino, M., Seno, S., and Tiepolo, L., 2009, U-Pb zircon ages for post-Variscan volcanism in the Ligurian Alps (northern Italy): Journal of the Geological Society of London, v. 166, p. 101–114, doi:10.1144/0016-76492008-027.

Deer, W.A., Howie, R.A., and Zussmann, J., 1992, An Introduction to Rock-Forming Minerals (2nd ed.): Essex, UK, Longman Scientific and Technical, 696 p.

Dumont, T., Schwartz, S., Guillot, S., Simon-Labric, T., Tricart, P., and Jourdan, S., 2012, Structural and sedimentary records of the Oligocene revolution in the western Alpine arc: Journal of Geodynamics, v. 56–57, p. 18–38, doi:10.1016/j.jog.2011.11.006.

Dunkl, I., Di Giulio, A., and Kuhlemann, J., 2001, Combination of single-grain fission-track chronology and morphological analysis of detrital zircon crystals in provenance studies—Sources of the Macigno Formation (Apennines, Italy): Journal of Sedimentary Research, v. 71, p. 516–525, doi:10.1306/102900710516.

Duretz, T., Gerya, T.V., and May, D.A., 2011, Numerical modelling of spontaneous slab breakoff and subsequent topographic response: Tectonophysics, v. 502, p. 244–256, doi:10.1016/j.tecto.2010.05.024.

Ehlers, T.A., Chaudhri, T., Kumar, S., Fuller, C.S., Willett, S.D., Ketcham, R.A., Brandon, M.T., Belton, D.X., Kohn, B.P., Gleadow, A.J.W., Dunai, T.J., and Fu, F.Q., 2005, Computational tools for low-temperature thermochronometer interpretation: Reviews in Mineralogy and Geochemistry, v. 58, p. 589–622, doi:10.2138/rmg.2005.58.22.

Elter, G., Elter, P., Sturani, C., Weidman, M., 1966, Sur la prolongation du domaine ligure de l'Apennin dans le Monferrat et les Alpes et sur l'origine de la Nappe de la Simme s. l. des Préalpes romande et chablaisiennes: Bulletin des Laboratoires de Géologie, Minéralogie, Géophysique et du Musée Géologique de l'Université de Lausanne, v. 167, p. 61–72.

Evans, M.J., and Mange-Rajetzky, M.A., 1991, The provenance of sediments in the Barrême thrust-top basin, Haute-Provence, France, *in* Morton, A.C., Todd, S.P., and Haughton, P.D.W., eds., Developments in Sedimentary Provenance Studies: Geological Society of London Special Publication 57, p. 323–342, doi:10.1144/GSL.SP.1991.057.01.24.

Evans, M.J., Elliott, T., Apps, G.M., and Mange-Rajetzky, M.A., 2004, The Tertiary Grés de Ville of the Barrême basin: Feather edge equivalent to the Grés d'Annot?, *in* Joseph, P., and Lomas S.A., eds., Deep-Water Sedimentation in the Alpine Basin of SE France: New Perspectives on the Gres D'Annot and Related Systems: Geological Society of London Special Publication 221, p. 97–110, doi:10.1144/GSL.SP.2004.221.01.06.

Féraud, G., Ruffet, G., Stephan, J.F., Lapierre, H., Delgado, E., and Popoff, M., 1995, Nouvelles données géochronologiques sur le volcanisme paléogène des Alpes occidentales: Marseille, Séance Spéciale de la Société Géologique de France et de l'Association des Géologues du SE "Magmatisme dans le sud-est de la France," p. 38.

Festa, A., Dela Pierre, F., Irace, A., Piana, F., Fioraso, G., Lucchesi, S., Boano, P., and Forno, M.G., 2011, Carta Geologica d'Italia, Foglio 156 Torino Est: Servizio Geologico del Italia, scale 1:50,000.

Ford, M., and Lickorish, W.H., 2004, Foreland basin evolution around the western Alpine Arc, *in* Joseph, P., and Lomas S.A., eds., Deep-Water Sedimentation in the Alpine Basin of SE France: New Perspectives on the Gres D'Annot and Related Systems: Geological Society of London Special Publication 221, p. 39–63, doi:10.1144/GSL.SP.2004.221.01.04.

Garver, J.I., Brandon, M.T., Roden-Tice, M., and Kamp, P.J.J., 1999, Exhumation history of orogenic highlands determined by detrital fission-track thermochronology, *in* Ring, U., Brandon, M.T., Lister, G.S., and Willett, S.D., eds., Exhumation Processes: Normal Faulting, Ductile Flow, and Erosion: Geological Society of London Special Publication 154, p. 283–304, doi:10.1144/GSL.SP.1999.154.01.13.

Garzanti, E., and Malusà, M.G., 2008, The Oligocene Alps: Domal unroofing and drainage development during early orogenic growth: Earth and Planetary Science Letters, v. 268, p. 487–500, doi:10.1016/j.epsl.2008.01.039.

Garzanti, E., Vezzoli, G., Lombardo, B., Ando, S., Mauri, E., Monguzzi, S., and Russo, M., 2004, Collision-orogen provenance (western Alps): Detrital signatures and unroofing trends: The Journal of Geology, v. 112, p. 145–164, doi:10.1086/381655.

Gebauer, D., Schmid, R., von Quadt, A., and Ulmer, P., 1992, Oligocene, Permian and Panafrican zircon ages from rocks of the Balmuccia Peridotite and of the Lower Layered Group in the Ivrea zone: Schweizerische Mineralogische und Petrographische Mitteilungen, v. 72, p. 113–122.

Gebauer, D., Schertl, H.P., Brix, M., and Schreyer, W., 1997, 35 Ma old ultrahigh-pressure metamorphism and evidence for very rapid exhumation in the Dora-Maira Massif, western Alps: Lithos, v. 41, p. 113–122, doi:10.1016/S0024-4937(97)82002-6.

Gidon, M., 1991, Notice Explicative de la Feuille de Gap à 1/50000: Carte Géologique 869: Orléans, France, BRGM Editions, scale 1:50,000.

Gidon, M., Monjuvent, G., Flandrin, J., Moullade, M., Durozoy, G., and Damiani, L., 1991, Notice Explicative de la Feuille Laragne-Montéglin à 1/50000: Carte Géologique 893: Orléans, France, BRGM Editions, scale 1:50,000.

Glotzbach, C., Bernet, M., and van der Beek, P., 2011, Detrital thermochronology records changing source areas and steady exhumation in the western and central European Alps: Geology, v. 39, p. 239–242, doi:10.1130/G31757.1.

Graciansky, P.C., Roberts, D.G., and Tricart, P., 2010, The Western Alps, From Rift to Passive Margin to Orogenic Belt: An Integrated Geoscience Overview; Developments in Earth Surface Processes: Amsterdam, Netherlands, Elsevier, 429 p.

Handy, M.R., Schmid, S.M., Bousquet, R., Kissling, E., and Bernoulli, D., 2010, Reconciling plate-tectonic reconstructions of Alpine Tethys with the geological-geophysical record of spreading and subduction in the Alps: Earth-Science Reviews, v. 102, p. 121–158, doi:10.1016/j.earscirev.2010.06.002.

Hunziker, J., Desmons, J., and Hurford, A.J., 1992, Thirty-Two Years of Geochronological Work in the Central and Western Alps: A Review on Seven Maps: Mémoires des Laboratoires de Géologie, Minéralogie, Géophysique et du Musée Géologique de l'Université de Lausanne 13, 59 p.

Jakes, P., and White, A.J.R., 1971, Composition of island arcs and continental growth: Earth and Planetary Science Letters, v. 12, p. 224–230, doi:10.1016/0012-821X(71)90081-1.

Jakes, P., and White, A.J.R., 1972, Major trace element abundances in volcanic rocks of orogenic areas: Geological Society of America Bulletin, v. 83, p. 29–40, doi:10.1130/0016-7606(1972)83[29:MATEAI]2.0.CO;2.

Jolivet, L., Faccenna, C., and Piromallo, C., 2009, From mantle to crust: Stretching the Mediterranean: Earth and Planetary Science Letters, v. 285, p. 198–209, doi:10.1016/j.epsl.2009.06.017.

Joseph, P., and Lomas, S.A., 2004, Deep-water sedimentation in the Alpine foreland basin of SE France, *in* Joseph, P., and Lomas S.A., eds., Deep-Water Sedimentation in the Alpine Basin of SE France: New Perspectives on the Gres D'Annot and Related Systems: Geological Society of London Special Publication 221, p. 1–16, doi:10.1144/GSL.SP.2004.221.01.01.

Jourdan, S., Bernet, M., Schwartz, S., Guillot, S., Tricart, P., Chauvel, C., Dumont, T., Montagnac, G., and Bureau, S., 2012, Tracing the Oligocene-Miocene Evolution of the Western Alps Drainage Divide with Pebble Petrology, Geochemistry, and Raman Spectroscopy of Foreland Basin Deposits: Journal of Geology, v. 120, no. 6, p. 603–624.

Kempf, O., Matter, A., Burbank, D.W., and Mange, M., 1999, Depositional and structural evolution of a foreland basin margin in a magnetostratigraphic framework: The eastern Swiss

Molasse basin: International Journal of Earth Sciences, v. 88, p. 253–275, doi:10.1007/s005310050263.
Köppel, V., 1974, Isotopic U-Pb ages of monazites and zircons from the crust-mantle transition and adjacent units of the Ivrea and Ceneri zones (southern Alps, Italy): Contributions to Mineralogy and Petrology, v. 43, p. 55–70, doi:10.1007/BF00384652.
Kuhlemann, J., 2000, Post-collisional sediment budget of circum-Alpine basins (Central Europe): Memorie degli Studi di Geologia e Mineralogia del Universita di Padova, v. 52, p. 1–91.
Kühni, A., and Pfiffner, O.A., 2001, Drainage patterns and tectonic forcing: A model study for the Swiss Alps: Basin Research, v. 13, p. 169–197, doi:10.1046/j.1365-2117.2001.00146.x.
Lardeaux, J.M., Schwartz, S., Tricart, P., Paul, A., Guillot, S., Bethoux, N., and Masson, F., 2006, A crustal-scale cross-section of the south-western Alps combining geophysical and geological imagery: Terra Nova, v. 18, p. 412–422, doi:10.1111/j.1365-3121.2006.00706.x.
Malusà, M.G., Villa, I.M., Vezzoli, G., and Garzanti, E., 2011a, Detrital geochronology of unroofing magmatic complexes and the slow erosion of Oligocene volcanoes in the Alps: Earth and Planetary Science Letters, v. 301, p. 324–336, doi:10.1016/j.epsl.2010.11.019.
Malusà, M.G., Faccenna, C., Garzanti, E., and Polini, R., 2011b, Divergence in subduction zones and exhumation of high pressure rocks (Eocene western Alps): Earth and Planetary Science Letters, v. 310, p. 21–32, doi:10.1016/j.epsl.2011.08.002.
Montenat, C., Leyrit, H., Gillot, P.Y., Janin, M.C., and Barrier, P., 1999, Extension du volcanisme oligocène dans l'arc de Castellane (chaînes subalpines de Haute-Provence): Géologie de la France, v. 1, p. 43–48.
Montgomery, D.R., and Brandon, M.T., 2002, Topographic controls on erosion rates in tectonically active mountain ranges: Earth and Planetary Science Letters, v. 201, p. 481–489, doi:10.1016/S0012-821X(02)00725-2.
Morag, N., Avigad, D., Harlavan, Y., McWilliams, M.O., and Michard, A., 2008, Rapid exhumation and mountain building in the western Alps: Petrology and $^{40}Ar/^{39}Ar$ geochronology of detritus from Tertiary basins of southeastern France: Tectonics, v. 27, p. TC2004, doi:10.1029/2007TC002142.
Mosca, P., Festa, A., Polino, R., Rogledi, S., and Rossi, M., 2007, Contesto strutturale e deposizionale della Collina di Torino alla terminazione occidentale dei thrusts Sudalpini: Rendiconti della Società Geologica Italiana, v. 4, p. 277–278.
Paquette, J.L., 1987, Comportement des Systèmes Isotopiques U-Pb et Sm-Nd dans le Métamorphisme Eclogitique: Chaîne Hercynienne et Chaîne Alpine [Ph.D. thesis]: Rennes, France, Université Rennes, 232 p.
Paquette, J.L., and Tiepolo, M., 2007, High resolution (5 µm) U-Th-Pb isotope dating of monazite with excimer laser ablation (ELA)-ICPMS: Chemical Geology, v. 240, p. 222–237, doi:10.1016/j.chemgeo.2007.02.014.
Paul, A., Cattaneo, M., Thouvenot, F., Spallarossa, D., Béthoux, N., and Fréchet, J., 2001, A three-dimensional crustal velocity model of the southwestern Alps from local earthquake tomography: Journal of Geophysical Research, v. 106, p. 19,367–19,389, doi:10.1029/2001JB000388.
Pfiffner, O.A., 1986, Evolution of the north Alpine foreland basin in the central Alps, *in* Allen, P.A., and Homewood, P., eds., Foreland Basins: International Association of Sedimentologists Special Publication 8, p. 219–228, doi:10.1002/9781444303810.ch11.
Pfiffner, O.A., Schlunegger, F., and Buiter, S.J.H., 2002, The Swiss Alps and their peripheral foreland basin: Stratigraphic response to deep crustal processes: Tectonics, v. 21, 1054, doi:10.1029/2002TC001465.
Piromallo, C., and Faccenna, C., 2004, How deep can we find the traces of Alpine subduction?: Geophysical Research Letters, v. 31, L06605, doi:10.1029/2003GL019288.
Polino, R., Ruffini, R., and Ricci, B., 1991, Le molasse terziare della collina di Torino: Atti Ticinensi Scienze, v. 34, p. 85–95.
Press, W.H., Teukolsky, S.A., Vetterling, W.T., and Flannery, B.P., 1992, Numerical Recipes in FORTRAN (2nd ed.): New York, Cambridge University Press, 963 p.
Rubatto, D., and Hermann, J., 2001, Exhumation as fast as subduction?: Geology, v. 29, p. 3–6, doi:10.1130/0091-7613(2001)029<0003:EAFAS>2.0.CO;2.
Schlunegger, F., and Simpson, G., 2002, Possible erosional control on lateral growth of the European central Alps: Geology, v. 30, p. 907–910, doi:10.1130/0091-7613(2002)030<0907:PECOLG>2.0.CO;2.
Schlunegger, F., Burbank, D.W., Matter, A., Engesser, B., and Modden, C., 1996, Magnetostratigraphic calibration of the Oligocene to middle Miocene (30–15 Ma) mammal biozones and depositional sequences of the Swiss Molasse basin: Eclogae Geologicae Helvetiae, v. 89, p. 753–788.
Schlunegger, F., Matter, A., Burbank, D.W., and Klaper, E.M., 1997, Magnetostratigraphic constraints on the relationship between evolution of the central Swiss Molasse basin and Alpine orogenic events: Geological Society of America Bulletin, v. 109, p. 225–241, doi:10.1130/0016-7606(1997)109<0225:MCORBE>2.3.CO;2.
Schmid, S.M., and Kissling, E., 2000, The arc of the western Alps in the light of geophysical data on deep crustal structure: Tectonics, v. 19, p. 62–85, doi:10.1029/1999TC900057.
Schmid, S.M., Fügenschuh, B., Kissling, E., and Schuster, R., 2004, Tectonic map and overall architecture of the Alpine orogen: Eclogae Geologicae Helvetiae, v. 97, p. 93–117, doi:10.1007/s00015-004-1113-x.
Schwartz, S., 2000, La Zone Piémontaise des Alpes Occidentales: Un Paléo-Complexe de Subduction. Arguments Métamorphiques, Géochronologiques et Structuraux: Lyon, France, Université Claude-Bernard Lyon I, 313 p.
Schwartz, S., Lardeaux, J.M., Guillot, S., and Tricart, P., 2000, The diversity of eclogitic metamorphism in the Monviso ophiolitic complex, western Alps, Italy: Geodinamica Acta, v. 13, p. 169–188, doi:10.1016/S0985-3111(00)00112-1.
Schwartz, S., Tricart, P., Lardeaux, J.M., Guillot, S., and Vidal, O., 2009, Late tectonic and metamorphic evolution of the Piedmont accretionary wedge (Queyras Schistes lustrés, western Alps): Evidences for tilting during Alpine collision: Geological Society of America Bulletin, v. 121, p. 502–518, doi:10.1130/B26223.1.
Schwartz, S., Guillot, S., Tricart, P., Bernet, M., Jourdan, S., Dumont, T., and Montagnac, G., 2012, Source tracing of detrital serpentinite in the Oligocene molasse deposits from western Alps (Barrême basin): Implications for relief formation in the internal zone: Geological Magazine, v. 149, p. 841–856, doi:10.1017/S0016756811001105.
Sinclair, H.D., 1997a, Flysch to molasse transition in peripheral foreland basins: The role of the passive margin versus slab breakoff: Geology, v. 25, p. 1123–1126, doi:10.1130/0091-7613(1997)025<1123:FTMTIP>2.3.CO;2.
Sinclair, H.D., 1997b, Tectonostratigraphic model for underfilled peripheral foreland basins: An Alpine perspective: Geological Society of America Bulletin, v. 109, p. 324–346, doi:10.1130/0016-7606(1997)109<0324:TMFUPF>2.3.CO;2.
Spiegel, C., Kuhlemann, J., Dunkl, I., Frisch, W., von Eynatten, H., and Balogh, K., 2000, The erosion history of the central Alps: Evidence from the zircon fission-track data of the foreland basin sediments: Terra Nova, v. 12, p. 163–170, doi:10.1046/j.1365-3121.2000.00289.x.
Spiegel, C., Kuhlemann, J., Dunkl, I., and Frisch, W., 2001, Paleogeography and catchment evolution in a mobile orogenic belt: The central Alps in Oligo–Miocene times: Tectonophysics, v. 341, p. 33–47, doi:10.1016/S0040-1951(01)00187-1.
Stewart, R.J., and Brandon, M.T., 2004, Detrital zircon fission-track ages for the "Hoh Formation": Implications for late Cenozoic evolution of the Cascadia subduction wedge: Geological Society of America Bulletin, v. 116, p. 60–75, doi:10.1130/B22101.1.
Sue, C., and Tricart, P., 2002, Widespread post-nappe normal faulting in the Internal Western Alps: A new constraint on arc dynamics: Journal of the Geological Society of London, v. 159, p. 61–70.
Sue, C., and Tricart, P., 2003, Neogene to ongoing normal faulting in the inner western Alps: A major evolution of the late alpine tectonics: Tectonics, v. 22, no. 5.
Tiepolo, M., 2003, In situ Pb geochronology of zircon with laser ablation–inductively coupled plasma–sector field mass spectrometry: Chemical Geology, v. 199, p. 159–177, doi:10.1016/S0009-2541(03)00083-4.
Tricart, P., and Schwartz, S., 2006, A north-south section across the Queyras Schistes lustrés (Piedmont zone, western Alps): Syn-collision refolding of a subduction wedge: Eclogae Geologicae Helvetiae, v. 99, p. 429–442, doi:10.1007/s00015-006-1197-6.
Tricart, P., and Sue, C., 2006, Faulted backfold versus reactivated backthrust: The role of inherited structures during late extension in the frontal Piémont nappes east of Pelvoux (western Alps): International Journal of Earth Sciences, v. 95, p. 827–840, doi:10.1007/s00531-006-0074-x.
Vermeesch, P., 2004, How many grains are needed for a provenance study?: Earth and Planetary Science Letters, v. 224, no. 3–4, p. 441–451.
Vernon, A.J., van der Beek, P.A., Sinclair, H.D., and Rahn, M.K., 2008, Increase in late Neogene denudation of the European Alps confirmed by analysis of a fission-track thermochronology database: Earth and Planetary Science Letters, v. 270, p. 316–329, doi:10.1016/j.epsl.2008.03.053.
Vezzoli, G., Garzanti, E., and Moguzzi, S., 2004, Erosion in the western Alps (Dora Baltea basin): 1. Quantifying sediment provenance: Sedimentary Geology, v. 171, p. 227–246, doi:10.1016/S0037-0738(04)00247-7.
Vignaroli, G., Faccenna, C., Jolivet, L., Piromallo, C., and Rossetti, F., 2008, Subduction polarity reversal at the junction between the western Alps and the Northern Apennines, Italy: Tectonophysics, v. 450, p. 34–50, doi:10.1016/j.tecto.2007.12.012.
von Blanckenburg, F., and Davies, J.H., 1995, Slab breakoff: A model for syncollisional magmatism and tectonics in the Alps: Tectonics, v. 14, p. 120–131, doi:10.1029/94TC02051.
von Blanckenburg, F., Villa, I.M., Baur, H., Morteani, G., and Steiger, R.H., 1989, Time calibration of a *PT*-path from the western Tauern Window, eastern Alps—The problem of closure temperatures: Contributions to Mineralogy and Petrology, v. 101, p. 1–11, doi:10.1007/BF00387196.
von Eynatten, H., and Wijbrans, J.R., 2003, Precise tracing of exhumation and provenance using $^{40}Ar/^{39}Ar$ geochronology of detrital white mica: The example of the central Alps, *in* McCann, T., and Saintot, A., eds., Tracing Tectonic Deformation Using the Sedimentary Record: Geological Society of London Special Publication 208, p. 289–305.
Wilson, M., 1989, Igneous Petrogenesis: A Global Tectonic Approach: London, Chapman and Hall, 466 p.

MANUSCRIPT RECEIVED 11 JULY 2012
REVISED MANUSCRIPT RECEIVED 30 NOVEMBER 2012
MANUSCRIPT ACCEPTED 1 DECEMBER 2012

Printed in the USA